iScience

CellPress

Article

Human Hyperekplexic Mutations in Glycine Receptors Disinhibit the Brainstem by Hijacking $GABA_A$ Receptors

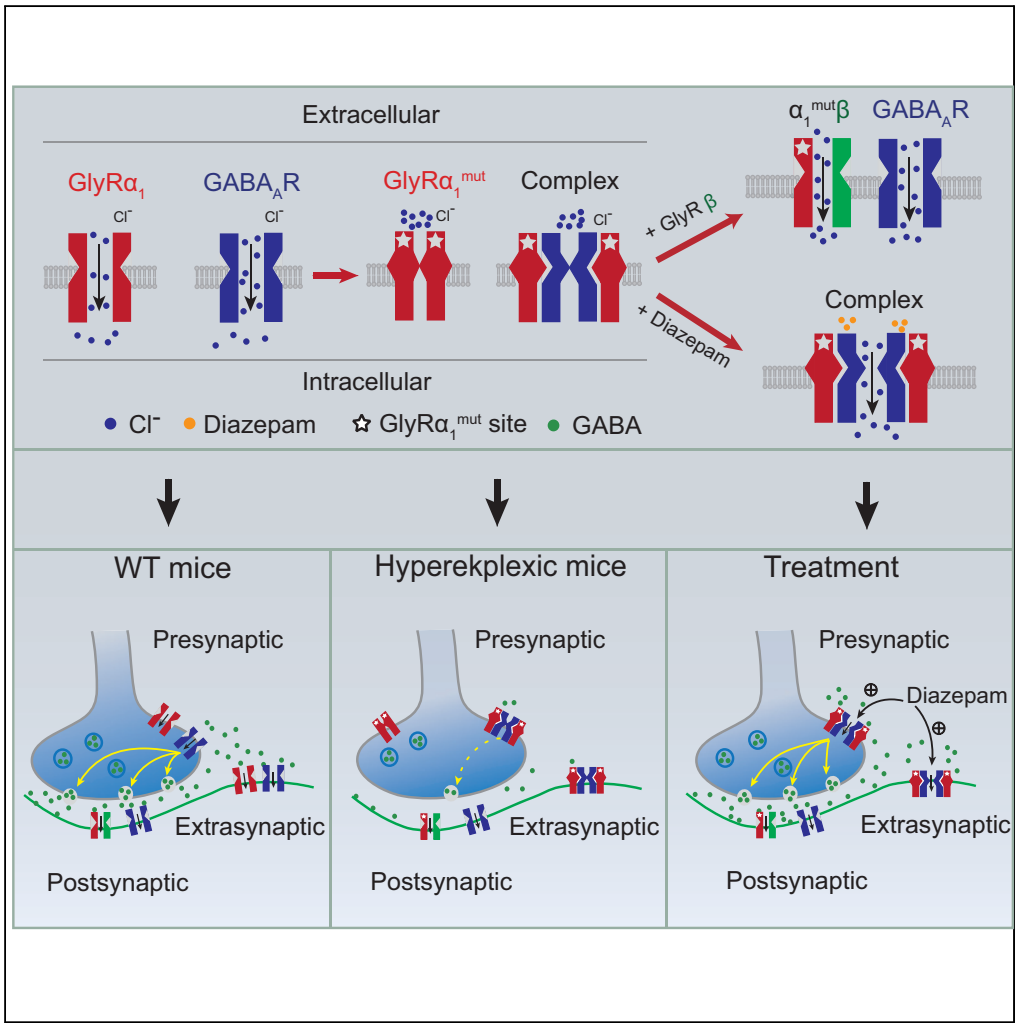

Guichang Zou, Qi Chen, Kai Chen, ..., Dan Liu, Li Zhang, Wei Xiong

wxiong@ustc.edu.cn

HIGHLIGHTS

Hyperekplexic mutant GlyRs interact with $GABA_ARs$ and disrupt the $GABA_AR$ function

Pre- and extra-synaptic $GABA_ARs$ are deficient in the hyperekplexia disease

α_5-Containing $GABA_AR$ is a potential therapeutic target for the hyperekplexia disease

Zou et al., iScience 19, 634–646
September 27, 2019
https://doi.org/10.1016/j.isci.2019.08.018

iScience

CellPress

Article

Human Hyperekplexic Mutations in Glycine Receptors Disinhibit the Brainstem by Hijacking $GABA_A$ Receptors

Guichang Zou,[1] Qi Chen,[1] Kai Chen,[1] Xin Zuo,[1] Yushu Ge,[1] Yiwen Hou,[1] Tao Pan,[1] Huilin Pan,[3] Dan Liu,[1] Li Zhang,[4] and Wei Xiong[1,2,5,*]

SUMMARY

Hyperekplexia disease is usually caused by naturally occurring point mutations in glycine receptors (GlyRs). However, the γ-aminobutyric acid type A receptor ($GABA_AR$) seems to be also involved regarding the therapeutic basis for hyperekplexia using benzodiazepines, which target $GABA_ARs$ but not GlyRs. Here, we show that the function of $GABA_ARs$ was significantly impaired in the hypoglossal nucleus of hyperekplexic transgenic mice. Such impairment appeared to be mediated by interaction between $GABA_AR$ and mutant GlyR. The $GABA_AR$ dysfunction was caused only by mutant GlyR consisting of homomeric α_1 subunits, which locate primarily at pre- and extra-synaptic sites. In addition, the rescue effects of diazepam were attenuated by Xli-093, which specifically blocked diazepam-induced potentiation on α_5-containing $GABA_AR$, a major form of pre- and extra-synaptic $GABA_AR$ in the brainstem. Thus, our results suggest that the pre- and extra-synaptic $GABA_ARs$ could be a potential therapeutic target for hyperekplexia disease caused by GlyR mutations.

INTRODUCTION

γ-Aminobutyric acid (GABA) and glycine are the major inhibitory neurotransmitters in the brain (Nemecz et al., 2016). Glycine receptor (GlyR) and GABA type A receptor ($GABA_AR$) are members of a large Cys-loop superfamily and are structurally similar ligand-gated ion channels (Langosch et al., 1990; Jacob et al., 2008). On activation, the GlyR and $GABA_AR$ selectively conduct Cl^- through central pores, leading to neuron hyperpolarization and inhibitory neurotransmission in the central nervous system (Nemecz et al., 2016). These receptors are usually localized at the synapse postsynaptically (Essrich et al., 1998; Langosch et al., 1988). Emerging evidence has suggested that certain isoforms of $GABA_AR$, including α_5 subunit-containing receptors, can be found pre-synaptically and extra-synaptically (Brickley and Mody, 2012; Castro et al., 2011; Delgado-Lezama et al., 2013; Jia et al., 2005; Hauser et al., 2005). GlyR is widely distributed in the central nervous system, particularly in the brainstem and spinal cord (Hruskova et al., 2012; Xiong et al., 2014). To date, four α-subunits ($\alpha_{1\text{-}4}$) and one β-subunit of GlyR have been identified. All GlyR α subunits can form functional homomeric channels that are mainly located on the pre- and extra-synaptic membrane of a synapse (Hruskova et al., 2012; Xiong et al., 2014; McCracken et al., 2017; Turecek and Trussell, 2001). However, after co-assembling with the α subunits, the β subunit can form functional post-synaptic heteromeric αβ channels (Pribilla et al., 1992; Xiong et al., 2014).

Hyperekplexia is a human genetic neurological disorder usually caused by point mutations in α_1 GlyRs (Shiang et al., 1993). Although rare, this disease can be life-threatening in children and is characterized by exaggerated startle response and muscle stiffness following an unexpected stimulus. Numerous point mutations in the GlyR α_1 subunit have been identified and characterized as hyperekplexic mutations disrupting GlyR function (Bode and Lynch, 2014). Among them, the R271Q was the most common dominant $GlyR\alpha_1$ mutation identified in patients with hyperekplexia (Thomas et al., 2013). Despite strong evidence suggesting that the point mutations in the α_1 GlyR are strongly associated with hyperekplexia, the primary therapeutic agent effectively used to treat hyperekplexia in humans is benzodiazepines (Dijk and Tijssen., 2010; Garg et al., 2008; Tijssen et al., 1997), which selectively enhances $GABA_AR$ functioning (Dray and Straughan, 1976; Macdonald and Barker, 1978). Thus, $GABA_ARs$ seems to be the primary therapeutic target in hyperekplexia. Consistently, a previous investigation revealed a deficiency in both glycinergic and GABAergic transmission in the spinal cord of R271Q mutant mice (Becker et al., 2002; Von Wegerer et al., 2003). Unfortunately, the cellular and molecular mechanisms underlying the $GABA_AR$ deficiency in

[1]Hefei National Laboratory for Physical Sciences at the Microscale, Neurodegenerative Disorder Research Center, School of Life Sciences, University of Science and Technology of China, Hefei 230026, China

[2]Center for Excellence in Brain Science and Intelligence Technology, Chinese Academy of Sciences, Shanghai 200031, China

[3]Center for Neuroscience and Pain Research, Department of Anesthesiology and Perioperative Medicine, The University of Texas MD Anderson Cancer Center, Houston, TX, USA

[4]Laboratory for Integrative Neuroscience, National Institute on Alcohol Abuse and Alcoholism, National Institutes of Health, Bethesda, MD, USA

[5]Lead Contact

*Correspondence: wxiong@ustc.edu.cn

https://doi.org/10.1016/j.isci.2019.08.018

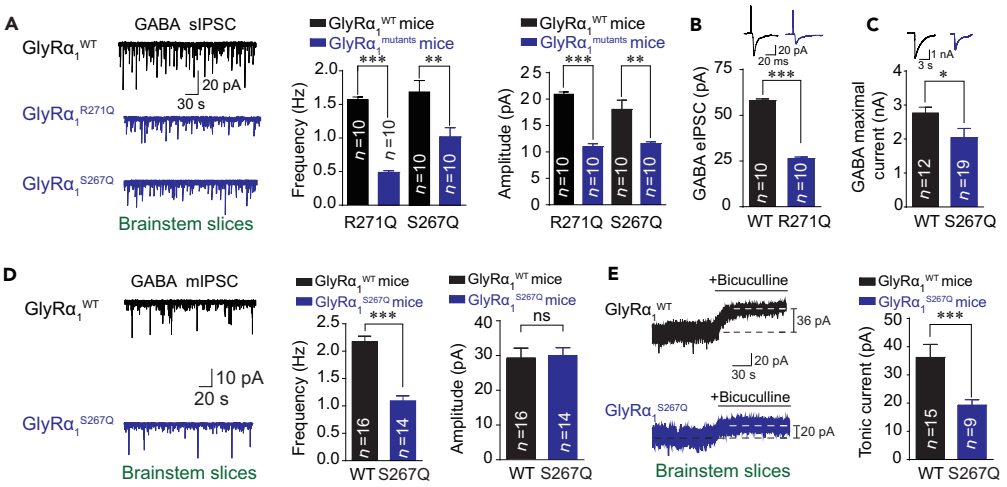

Figure 1. Dysfunction of GABA$_A$Rs in the Hyperekplexic Mutant Mice

(A) Trace records, average frequency, and amplitude of GABAergic sIPSCs in brainstem hypoglossal nucleus slices from WT, GlyRα$_1^{R271Q}$, and GlyRα$_1^{S267Q}$ mutant mice.

(B) Trace records and average amplitude of GABAergic eIPSCs in brainstem hypoglossal nucleus slices from WT and GlyRα$_1^{R271Q}$ mutant mice.

(C) Trace records and average values of GABA maximal current induced by puffing 1 mM GABA in brainstem hypoglossal nucleus slices from WT and GlyRα$_1^{S267Q}$ mutant mice.

(D) Trace records, average frequency, and amplitude of GABAergic mIPSCs in brainstem hypoglossal nucleus slices from WT and GlyR α$_1^{S267Q}$ mutant mice.

(E) Trace records and average values of BSTC in brainstem hypoglossal nucleus slices from WT and GlyRα$_1^{S267Q}$ mutant mice.

All digits within the columns represent numbers of cells measured from at least three mice. Data are represented as mean ± SEM. *p < 0.05, **p < 0.01, ***p < 0.001 based on unpaired t tests; ns, not significant (p > 0.05).

hyperekplexia remains unclear. Such deficiency is not caused by the posttranslational modification of either GlyR or GABA$_A$R protein since radioligand binding to these receptors was unaffected (Becker et al., 2002). The speculation that GlyR can cross-talk or interact with GABA$_A$R has been long-standing (Wojcik et al., 2006). These receptors are abundant in the spinal cord and brainstem where the neurotransmitters GABA and glycine are colocalized and co-released from the same vesicles at many motoneuron synapses (Jonas et al., 1998). Strong evidence suggests that a substantial proportion of spinal cord inhibitory synapses host both GlyRs and GABA$_A$Rs. Nevertheless, direct evidence and the *in vivo* consequence of the potential GlyR-GABA$_A$R interaction have not been reported. Considering these questions, we conducted experiments using various approaches to explore the nature of the interaction through which hyperekplexic mutations in the GlyR α$_1$ subunits disrupt GABA$_A$R functioning at synapses.

RESULTS

GABA$_A$Rs Deficiency in the Brainstem of Hyperekplexic Mutant Mice

To determine whether the hyperekplexic point mutations in the α$_1$ GlyR could affect GABAergic transmission, we measured GABA release and GABA$_A$R functioning using patch clamp recording in the hypoglossal nucleus slices from two transgenic mouse lines carrying GlyRα$_1$ R271Q and S267Q hyperekplexic point mutations. Another mouse line carrying GlyRα$_1$ M287L point mutation was set as a negative control since this mutation was not found in patients with hyperekplexia and has been previously shown to scarcely change the function of GlyR in mice (Bode and Lynch, 2014; Xiong et al., 2014). Both the frequency and amplitude of GABAergic spontaneous inhibitory postsynaptic currents (sIPSCs) were remarkably attenuated in the hypoglossal nucleus of GlyRα$_1^{R271Q}$ and GlyRα$_1^{S267Q}$ but not in GlyRα$_1^{M287L}$ mutant mice (Figures 1A and S1). Consistently, the electrical stimulation-evoked GABAergic IPSCs (eIPSCs) and the puffing GABA-induced currents were both significantly reduced in the GlyRα$_1^{R271Q}$ and GlyRα$_1^{S267Q}$ mutant mice (Figures 1B and 1C).

Next, we separately examined the function of GABA$_A$Rs at various synaptic locations including the pre-, post-, and extra-synapses. Here the GlyRα$_1^{S267Q}$ mice were used as a representative. The frequency but not the amplitude of the GABAergic mIPSCs was significantly decreased in the brainstem hypoglossal nucleus of

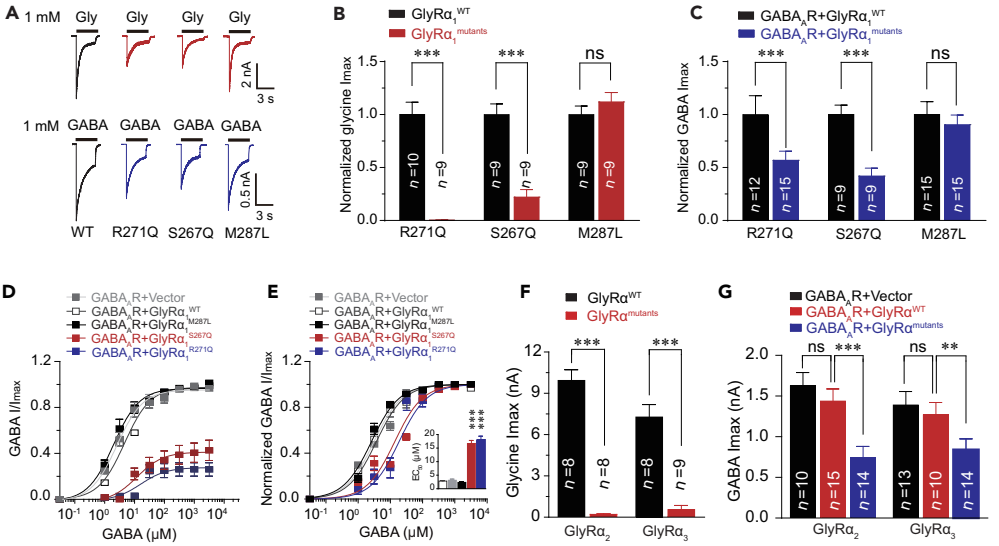

Figure 2. Impairment in $GABA_AR$s by Hyperekplexic GlyR α_1 Mutations in HEK-293 Cells

(A) Representative trace records of glycine I_{max} (up) and GABA I_{max} (down) separately induced by 1 mM glycine and GABA in HEK-293 cells co-expressing $GABA_AR$s ($\alpha_1\beta_2\gamma_2$) and various hyperekplexic mutant α_1 GlyRs.

(B) The average values of glycine I_{max} induced by 1 mM glycine in HEK-293 cells co-expressing $GABA_AR$s ($\alpha_1\beta_2\gamma_2$) and various hyperekplexic mutant α_1 GlyRs. The data were normalized to the I_{max} of the $GlyR\alpha_1^{WT}$ group.

(C) Average values of GABA I_{max} induced by 1 mM GABA in HEK-293 cells co-expressing $GABA_AR$s and various hyperekplexic mutant α_1 GlyRs. The data were normalized to their respective controls ($GlyR\alpha_1^{WT}$ group).

(D and E) Dose-response curves of I_{GABA} in HEK-293 cells co-expressing $GABA_AR$s ($\alpha_1\beta_2\gamma_2$) and either WT, α_1^{R271Q}, α_1^{S267Q}, or α_1^{M287L} GlyRs. The data were normalized to I_{max} of the $GlyR\alpha_1^{WT}$ group (D) or its own group (E).

(F) The average values of glycine I_{max} in HEK-293 cells expressing WT or α_2^{R305Q} or α_3^{R320Q} GlyRs.

(G) The average values of GABA I_{max} in HEK-293 cells co-expressing $GABA_AR$s ($\alpha_1\beta_2\gamma_2$) and WT or α_2^{R305Q} or α_3^{R320Q} GlyRs.

All digits within the columns represent numbers of cells measured. Data are represented as mean ± SEM. **p < 0.01, ***p < 0.001 based on unpaired t tests; ns, not significant (p > 0.05).

the $GlyR\alpha_1^{S267Q}$ mice compared with that in the wild-type (WT) littermates (Figure 1D). This suggests that a pre- but not post-synaptic impairment exists in GABAergic transmission. Then, we tested the bicuculline-sensitive tonic current (BSTC), which represents extra-synaptic $GABA_AR$ activity. The amplitude of the BSTC was also significantly reduced in the $GlyR\alpha_1^{S267Q}$ mice compared with that in the WT littermates (Figure 1E).

Hyperekplexic GlyRα_1 Mutations Cause $GABA_AR$ Deficiency when Co-expressed in HEK-293 Cells

Mutant GlyRs may disrupt the function of $GABA_AR$s in the same neuron since the preponderance of evidence has indicated a wide colocalization of GlyRs and $GABA_AR$s in brainstem neurons (Muller et al., 2004, 2006; Lorenzo et al., 2006, 2007; Waldvogel et al., 2019). Next, we investigated whether the $GlyR\alpha_1$ mutations could induce $GABA_AR$ deficiency if these receptors were co-expressed in HEK-293 cells. The $GlyR\alpha_1^{R271Q}$ and $GlyR\alpha_1^{S267Q}$ hyperekplexic point mutations significantly reduced the maximal amplitudes of the current (I_{max}) activated by puffing glycine (Figures 2A and 2B) and GABA (Figures 2A and 2C). $GlyR\alpha_1^{R271Q}$ and $GlyR\alpha_1^{S267Q}$, but not $GlyR\alpha_1^{M287L}$, mutations shifted the dose-response curve of the GABA current to the right (Figures 2D and 2E) and increased the half-maximal effective concentration (EC_{50}) values of the $GABA_AR$s (Figure 2E). Interestingly, the other two GlyR α subunits, including α_2 and α_3, exhibited the same characteristics as α_1 subunit in impairing $GABA_AR$ functions. For instance, the point mutations in the $GlyR\alpha_2$ (R305Q) and $GlyR\alpha_3$ (R320Q) subunits corresponding to R271Q of $GlyR\alpha_1$ not only reduced the glycine I_{max} (Figure 2F) when expressed alone but also inhibited GABA I_{max} when co-expressed with $GABA_AR$s (Figure 2G).

At high concentrations, GABA can also activate GlyRs (Figure S2) (Singer, 2008). Thus, we examined the efficacy of muscimol, which is a full agonist specific for $GABA_AR$ but not GlyR (Snodgrass, 1978) (Figure S3A), in activating $GABA_AR$-GlyR complexes. Consistent with our observation in the above-mentioned

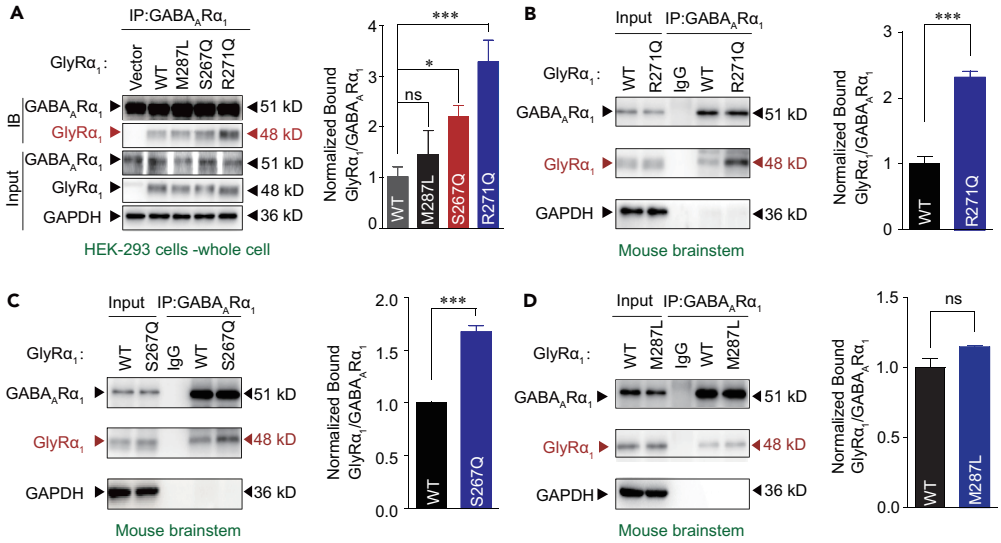

Figure 3. Identification of Interaction between GABA$_A$R and Hyperekplexic Mutant GlyRs

(A) GlyRα$_1$ was purified using GABA$_A$R α$_1$ antibodies in HEK-293 cells co-expressing GABA$_A$Rs ($\alpha_1\beta_2\gamma_2$) and WT/mutant α$_1$ GlyRs, and the co-precipitating proteins were detected by immunoblotting. Inputs are immunoblots of the same protein in cell lysates before Co-IP. Quantification of WT and mutant GlyR α$_1$ binding to GABA$_A$R α$_1$ subunits (n = 3). The data were normalized to the WT group.

(B and C) Endogenous brainstem GlyRα$_1$ of WT and GlyRα$_1$ R271Q (B) or S267Q (C) KI mice was purified using GABA$_A$R α$_1$ antibodies, and the co-precipitating proteins were detected by immunoblotting. Inputs are immunoblots of the same protein in tissue lysates before Co-IP. Quantification of WT and R271Q (B) or S267Q (C) mutant GlyRα$_1$ binding to GABA$_A$Rα$_1$ (n = 3 mice).

(D) Endogenous brainstem GlyRα$_1$ of WT and GlyRα$_1$ M287L KI mice was purified using GABA$_A$R α$_1$ antibodies, and the co-precipitating proteins were detected by immunoblotting. Inputs are immunoblots of the same protein in tissue lysates before Co-IP. Quantification of WT and M287L mutant GlyRα$_1$ binding to GABA$_A$Rα$_1$ (n = 3 mice). The data were normalized to the WT group.

Data are represented as mean ± SEM. *p < 0.05, ***p < 0.001 based on unpaired t tests; ns, not significant (p > 0.05).

experiments using GABA, the amplitude of muscimol (100 μM)-induced maximal current (I_{max}) was also significantly decreased in HEK-293 cells co-expressing GABA$_A$Rs with GlyRα$_1^{R271Q}$ or GlyRα$_1^{S267Q}$ (Figure S3B).

The Protein-Protein Interactions between GABA$_A$R and Hyperekplexic Mutant GlyR

First, we investigated whether the hyperekplexic mutations will affect the membrane trafficking of GlyR and GABA$_A$R. The western-blotting results showed that both the S267Q and R271Q point mutations in the GlyRα$_1$ subunit did not affect the protein expression level of GlyR or GABA$_A$R in plasma membranes extracted from HEK-293 cells co-transfected with the cDNA of GlyRα$_1^{WT}$, GlyRα$_1^{R271Q}$, and GlyRα$_1^{S267Q}$ with or without GABA$_A$Rs (Figure S4).

A possible mechanism of the GABA$_A$R deficiency in the presence of mutant GlyRs is that there may exist an interaction between GlyR and GABA$_A$R proteins. To test this hypothesis, we conducted a co-immunoprecipitation (Co-IP) assay of mutant or WT GlyRα$_1$ subunits and GABA$_A$Rs ($\alpha_1\beta_2\gamma_2$) co-expressed in HEK-293 cells. The point mutations R271Q and S267Q, but not M287L, significantly increased the amount of GlyR protein co-immunoprecipitated with GABA$_A$R proteins from whole cell lysates (Figures 3A, S5, and S6) and plasma membrane preparations (Figure S7). Similar results were observed *in vivo* in transgenic mice carrying GlyRα$_1$ mutations. The association between the GlyRs and GABA$_A$Rs was remarkably enhanced in the brainstem of the GlyRα$_1^{R271Q}$ (Figures 3B and S8A–S8C) and GlyRα$_1^{S267Q}$ (Figures 3C and S8D–S8F), but not GlyRα$_1^{M287L}$, mutant mice (Figures 3D and S8G–S8I).

The Site R271 Is Critical for the Interaction between GABA$_A$R and Hyperekplexic Mutant GlyR

Subsequently, we conducted a molecular dynamic simulation to evaluate the interaction between the subunits of GABA$_A$Rs (Miller and Aricescu, 2014) and hyperekplexic mutant GlyR subunits (Huang et al., 2017) in

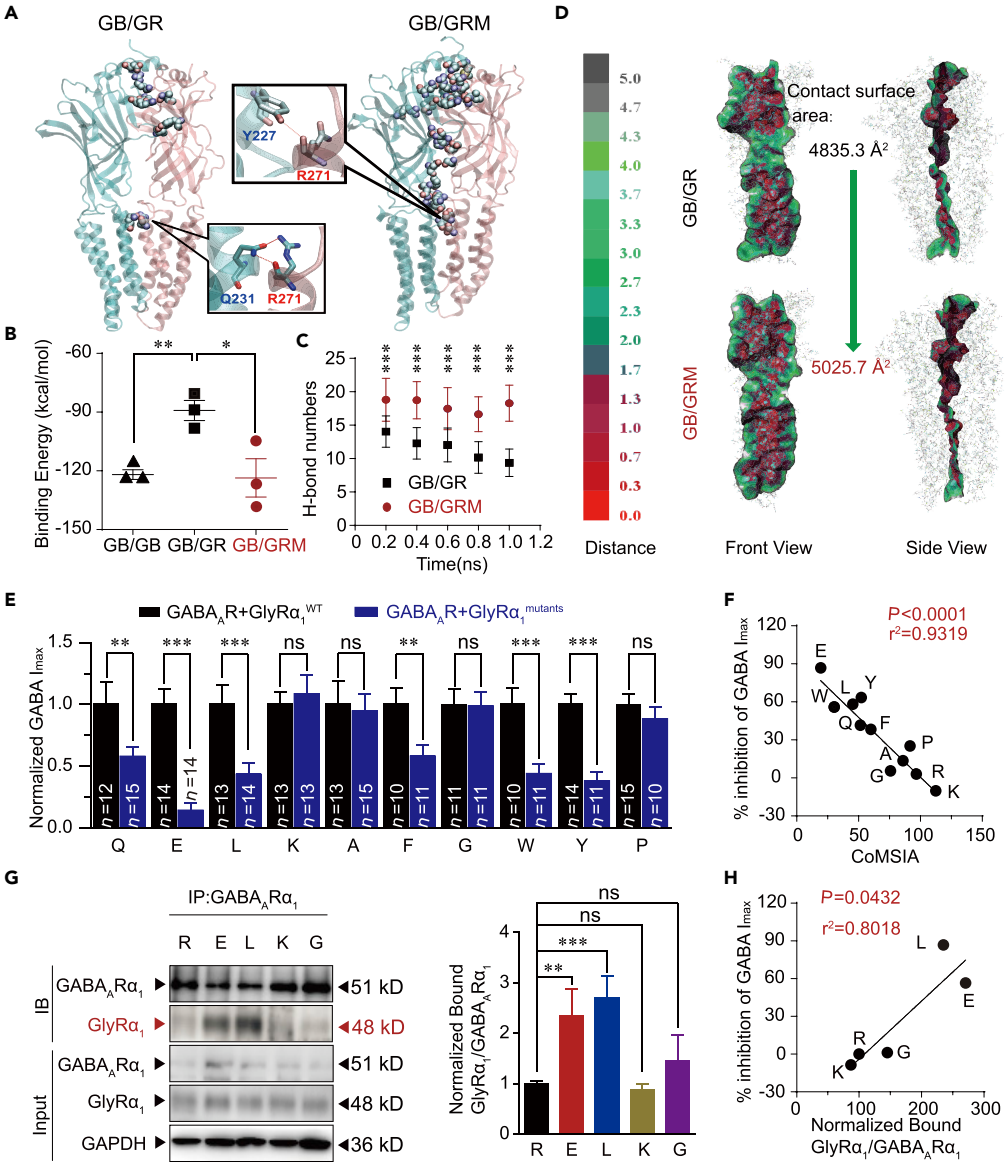

Figure 4. Molecular Dynamic Simulation, Mutagenesis, and Correlation Analysis

(A) Overview of residues forming H-bond between GB chain and GR chain in the GB/GR and GB/GRM complexes at the end of the simulation. GB chain and residue labels are colored in cyan. GR chain and residue labels are colored in pink. H-bonds are shown by the red dashed line.

(B) Binding energy (kcal/mol) between subunits in various composing form of dimers.

(C) Number of H-bonds formed between GB chain and GR chain in the GB/GR and GB/GRM complexes. The data are shown as averages of each 200 ps. Data are represented as mean ± SD.

(D) VDW contact surface between GB chain and GR chain in the GB/GR and GB/GRM complexes. Proteins are displayed in lines. Contact surfaces were mapped and colored according to the distances between two chains.

(E) Average values of GABA I_{max} induced by 1 mM GABA in HEK-293 cells co-expressing $GABA_AR$s and various R271 site mutant GlyR α_1 subunits. All data were normalized to their respective controls (WT group).

(F) Correlation analysis of CoMSIA values of various amino acids at 271 and the percentage inhibition of GABA I_{max}.

(G) GlyRα_1 was purified using $GABA_AR$ α_1 antibodies in HEK-293 cells co-expressing $GABA_AR$s ($\alpha_1\beta_2\gamma_2$) and GlyRα_1 carrying various R271 mutations, and the co-precipitating proteins were detected by immunoblotting. Inputs are immunoblots of the same protein in cell lysates before Co-IP. Quantification of WT and R271 mutant GlyRα_1 binding to $GABA_AR$ α_1 (n = 3). Data were normalized to the WT group.

Figure 4. *Continued*

(H) Correlation analysis of the percentage decrease in GABA I_{max} and amount of R271 mutant α_1 GlyRs co-immunoprecipitated with $GABA_AR$s.

All digits within the columns represent numbers of cells measured. Data are represented as mean ± SEM. **p < 0.01, ***p < 0.001 based on unpaired t tests; ns, not significant (p > 0.05).

different combinations of dimers. First, all simulations were reliable since no unexpected collapse of protein structures were observed (Figure S9). Then, the binding affinities between the subunits in the dimers, including $GABA_AR$ homer-dimers (GB/GB) and $GABA_AR$ bound with GlyR (GB/GR) or GlyR mutant (GB/GRM), were analyzed and compared. Among the WT receptor combinations, two subunits in the GB/GB complex showed the strongest binding affinity with a binding free energy (BFE) of −121.9 ± 4.3 kcal/mol. However, the binding affinities in the GB/GR complex were much weaker (−89.2 ± 8.9 kcal/mol). A significant decrease in BFE was observed between the subunits in GB/GRM (Figure 4B). Notably, the BFE value in GB/GRM was as low as −123.4 ± 14.3 kcal/mol, which is highly similar to the value observed in GB/GB. Further analysis indicates that the mutation of R271Q may lead to hydrogen bonding with TYR227 instead of GLN231 on $GABA_AR$ (Figure 4A). The R271Q mutation promotes a conformational change in the GB and GR subunits, leading to more intensive H-bond formation and a larger contact surface area between the subunits (Figures 4C and 4D).

To obtain further molecular insight into the role of site R271 in the association between $GABA_AR$s and GlyRs, we used mutagenesis to analyze the interrelationship between the function of $GABA_AR$s and the biophysical properties of the amino acid residue at 271 of the GlyRα_1. The mutation-induced decrease in glycine I_{max} (Figure S10A) and GABA I_{max} (Figure 4E) varied substantially. No correlation was observed between the percentage inhibition of glycine I_{max} and that of GABA I_{max} (Figure S10B), suggesting that the dysfunction in $GABA_AR$ does not depend on the efficacious levels of GlyRs. Then, to examine the biophysical properties of the amino acid residue at 271 of the GlyRα_1, we performed a comparative molecular similarity index analysis (CoMSIA), which is a comprehensive method evaluating polarity, electrostatic potential, and steric property. A strong correlation was observed between the CoMSIA values of various amino acids at 271 and the function of GlyRs (Figure S10C) or $GABA_AR$s (Figure 4F). Combined with the results of the molecular dynamics simulation, the R271Q point mutation likely suppresses the function of GlyR by altering the protein conformational change required for channel gating. This point mutation also disrupted $GABA_AR$ functioning by enhancing the interaction between GlyR and $GABA_AR$. To further test this hypothesis, we performed a Co-IP assay to examine the interaction between the mutant R271E/L/K/G α_1 GlyRs and $GABA_AR$s co-expressed in HEK-293 cells. Both the GlyRα_1 subunits and $GABA_AR\alpha_1$ subunits were identified in the co-immunoprecipitants pulled down by the $GABA_AR\alpha_1$ antibodies (Figures 4G and S11A–S11C). Among the four GlyRα_1 R271 mutations, the R271L and R271E mutations appeared to enhance the binding of GlyR to $GABA_AR$. The protein levels of GlyRα_1^{R271X} bound to $GABA_AR\alpha_1$ were significantly and positively correlated with the extent of the $GABA_AR$ deficiency, although their levels substantially varied (Figure 4H).

GlyR β Subunits Restore Dysfunction of $GABA_AR$s Caused by GlyR α_1 Mutations

The above-mentioned results have suggested that the pre- and extra- but not post-synaptic $GABA_AR$s were impaired in hyperekplexia disease. It is worth mentioning that GlyR homomers (α/α) have been found to primarily reside at pre/extra-synaptic sites, whereas GlyR heteromers (α/β) are mostly post-synaptic (Betz et al., 1991; Hruskova et al., 2012; Xiong et al., 2014; McCracken et al., 2017; Turecek and Trussell, 2001). Thus, a possible scenario is that different combinations of GlyR subunits may have distinct abilities to interact with $GABA_AR$s. To test this hypothesis, we performed the electrophysiological experiments and Co-IP assay. Addition of the GlyR β subunit indeed prevents the hyperekplexic point mutations in the α_1 subunit from hijacking the $GABA_AR$s because no functional disruption in the $GABA_AR$ was observed after co-expressing the GlyR β subunits with the GlyRα_1^{R271Q}/$GABA_AR$ complexes in HEK-293 cells (Figures 5A and 5B). Furthermore, the GlyR β subunits also significantly interrupted the association between the mutant α_1 GlyRs and $GABA_AR$s in HEK-293 cells (Figures 5C and S12). These observations may hint at why only pre- and extra-synaptic $GABA_AR$s have been impaired in hyperekplexia.

Colocalization and Interaction of α_5-Containing $GABA_AR$s and Hyperekplexic Mutant GlyRs

Emerging evidence suggests that α_5 subunits-containing $GABA_AR$ ($\alpha_5\beta_x\gamma_x$) is the primary form of pre- and extra-synaptic $GABA_AR$s in several brain regions, including the hippocampus, spinal cord, and brainstem (Brickley and Mody, 2012; Castro et al., 2011; Delgado-Lezama et al., 2013; Jia et al., 2005). Genetic deletion

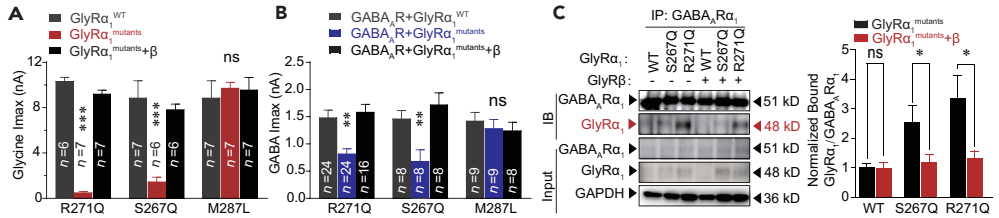

Figure 5. GlyR β Subunits Restore $GABA_ARs$ Functioning by Interrupting the Interaction between $GABA_AR\alpha_1$ and $GlyR\alpha_1$ Subunits

(A) Average glycine I_{max} values in HEK-293 cells co-expressing $GABA_ARs$ ($\alpha_1\beta_2\gamma_2$) and either homomeric or heteromeric hyperekplexic mutant α_1/β GlyRs.

(B) Average GABA I_{max} values in HEK-293 cells co-expressing $GABA_ARs$ ($\alpha_1\beta_2\gamma_2$) and either homomeric or heteromeric hyperekplexic mutant α_1/β GlyRs.

(C) $GlyR\alpha_1$ was purified using $GABA_AR$ α_1 antibodies in HEK-293 cells co-expressing $GABA_ARs$ ($\alpha_1\beta_2\gamma_2$) and homomeric or heteromeric hyperekplexic mutant α_1/β GlyRs, and the co-precipitating proteins were detected by immunoblotting. Inputs are immunoblots of the same protein in cell lysates before Co-IP. Quantification of WT and mutant $GlyR\alpha_1$ binding to $GABA_AR$ α_1 (n = 3). Data were normalized to the WT group.

All digits within the columns represent numbers of cells measured. Data are represented as mean ± SEM. *$p < 0.05$, **$p < 0.01$, ***$p < 0.001$ based on unpaired t tests; ns, not significant ($p > 0.05$).

of α_5-containing $GABA_A$ receptor could also cause severe convulsive seizure (Galanopoulou, 2008). Here, using RNAscope techniques, we conducted *in situ* hybridization and observed a high degree of colocalization of $GlyR\alpha_1$ and $GABA_AR\alpha_5$ subunit mRNAs in neurons in the hypoglossal nucleus of the brainstem in both the $GlyR\alpha_1^{S267Q}$ and WT mice (Figures 6A, 6B, and S13). Therefore, we next examined whether the hyperekplexic mutant GlyRs could also affect the α_5-containing $GABA_ARs$. The GABA I_{max} was significantly decreased when the α_1^{S267Q} mutant GlyRs were co-expressed with $\alpha_5\beta_2\gamma_2$ $GABA_ARs$ in HEK-293 cells (Figure 6C). Compared with the WT, the S267Q point mutation significantly increased the amount of GlyRs co-immunoprecipitated with $\alpha_5\beta_2\gamma_2$ $GABA_ARs$ in both the HEK-293 cells (Figures 6D and S14A–S14C) and the brainstem of $GlyR\alpha_1^{S267Q}$ mutant mice (Figures 6E and S14D–S14F).

Pre- and Extra-synaptic α_5-Containing $GABA_AR$ Is a Therapeutic Target of Diazepam for Hyperekplexia Disease

Benzodiazepines (BZDs) have always been used as the first-line medication to treat patients with hyperekplexia in the clinic (Dijk and Tijssen, 2010; Garg et al., 2008; Tijssen et al., 1997). Therefore, we next assessed whether diazepam (DIA), the most common BZD, could rescue the pre- and extra-synaptic $GABA_AR$ deficiency in the brainstem hypoglossal nucleus of $GlyR\alpha_1^{S267Q}$ KI mice. We conducted the following electrophysiological recordings, Co-IP experiments, and behavioral tests using homozygous and heterozygous $GlyR\alpha_1^{S267Q}$ KI mice because most $GlyR\alpha_1^{R271Q}$ KI mice died within 2–3 weeks (Figure S15). DIA significantly rescued the reduced frequency of GABA mIPSCs (Figure 7A) and the attenuated amplitude of the BSTC (Figure 7B) in the brainstem hypoglossal nucleus of the $GlyR\alpha_1^{S267Q}$ mutant mice. Consistently, DIA also significantly restored the attenuated GABA I_{max} in HEK-293 cells co-expressing α_5-containing $GABA_ARs$ and α_1^{S267Q} GlyRs (Figure S17A). These effects of DIA were remarkably diminished by Xli-093 (Figures 7A and 7B), which could specifically block DIA-induced potentiation on α_5- (Figure S16) but not α_1/α_2-containing $GABA_ARs$ (Clayton et al., 2015) (Figures S17B and S17C).

Next, we investigated whether the restoration of pre- and extra-synaptic $GABA_AR$ functioning by DIA in the brainstem hypoglossal nucleus was sufficient to treat hyperekplexia. An intraperitoneal (i.p.) injection of DIA markedly alleviated hind feet clenching behaviors and exaggerated tremors in the $GlyR\alpha_1^{S267Q}$ KI mice when the animals were picked up by their tails (Figure 7C). The therapeutic effect of DIA was completely abolished by an intra-brainstem hypoglossal nucleus microinjection of Xli-093 (Figure 7C). The $GlyR\alpha_1^{S267Q}$ mutant mice displayed exaggerated startle reflexes in response to various acoustic stimuli (Figure 7D). The systemic administration of DIA significantly inhibited the exaggerated startle responses of the $GlyR\alpha_1^{S267Q}$ KI mice. This DIA therapeutic effect was remarkably suppressed by an intra-brainstem hypoglossal nucleus injection of Xli-093 (Figure 7E). The startle reactions of the WT and various hyperekplexic mutant mice were significantly correlated with their brainstem hypoglossal nucleus presynaptic $GABA_ARs$ deficiency (expressed as percentage decreases in mIPSC frequency) and the bonding strength between the GlyR and $GABA_AR$ (expressed as normalized GlyR-$GABA_AR$ CO-IP) (Figure 7F). Altogether, our results

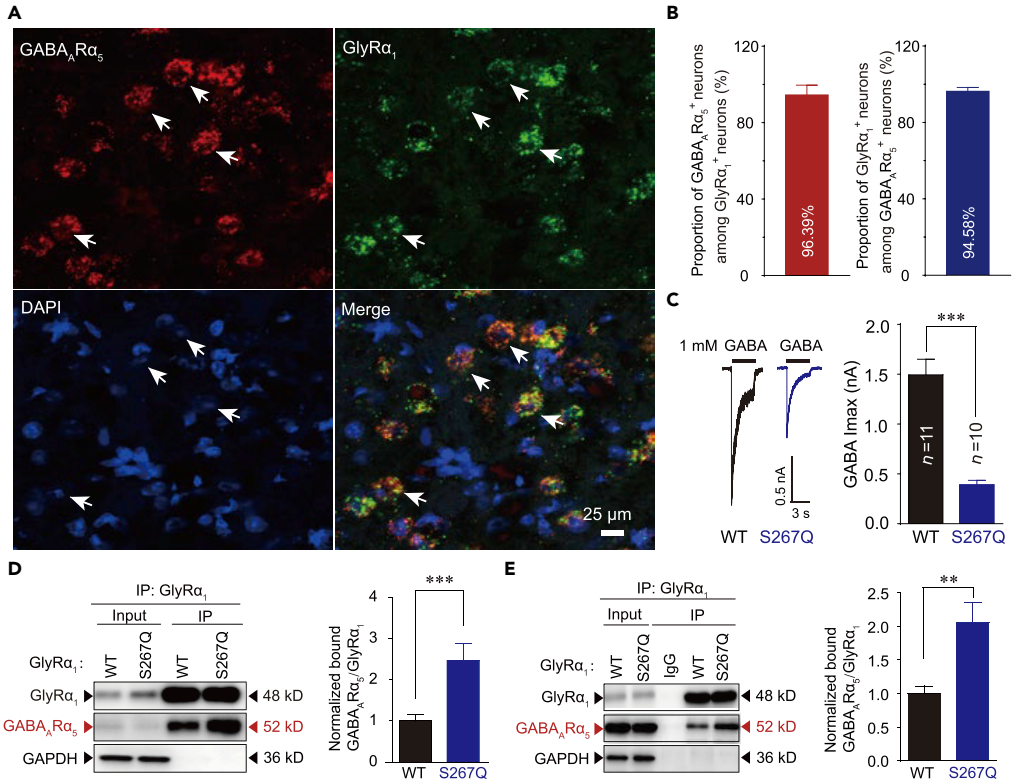

Figure 6. Interaction between α_5-Containing GABA$_A$R and Hyperekplexic Mutant GlyR

(A) Representative confocal imaging showing the colocalization of GABA$_A$Rα_5 and GlyRα_1 subunit mRNAs in the GlyRα_1^{S267Q} mouse brainstem using RNAscope technology (scale bar, 25 μm).

(B) Left, percentage of GlyRα_1 mRNA–positive neurons that co-express GABA$_A$Rα_5 mRNA. Right, percentage of GABA$_A$Rα_5 mRNA–positive neurons that co-express GlyRα_1 mRNA (n = 3 mice).

(C) Trace records and average values of GABA I_{max} activated by 1 mM GABA in HEK-293 cells co-expressing GABA$_A$Rs ($\alpha_5\beta_2\gamma_2$) and WT or α_1^{S267Q} mutant GlyRs. The digits within the columns represent numbers of cells measured.

(D) GABA$_A$Rα_5 was purified using GlyRα_1 antibodies in HEK-293 cells co-expressing GABA$_A$Rs ($\alpha_5\beta_2\gamma_2$) and WT/S267Q mutant GlyRα_1, and the co-precipitating proteins were detected by immunoblotting. Inputs are immunoblots of the same protein in cell lysates before Co-IP. Quantification of GABA$_A$R α_5 binding to WT and S267Q mutant GlyR α_1 (n = 3 mice).

(E) Endogenous brainstem GABA$_A$R α_5 in WT and GlyRα_1 S267Q KI mice were purified using GlyRα_1 antibodies, and the co-precipitating proteins were detected by immunoblotting. Inputs are immunoblots of the same protein in tissue lysates before Co-IP. Quantification of mouse brainstem GABA$_A$R α_5 binding to WT and S267Q mutant GlyR α_1 (n = 3 mice).

Data are represented as mean ± SEM. **p < 0.01, ***p < 0.001 based on unpaired t tests; ns, not significant (p > 0.05).

reveal that the pre- and extra-synaptic α_5-containing GABA$_A$R may be the major acting target of BDZ to treat hyperekplexia disease.

DISCUSSION

Both GABA$_A$R and GlyR mediate rapid synaptic transmissions in the central nervous system (Jacob et al., 2008; Langosch et al., 1990). Despite the widespread speculation that cross talk exists between these two types of receptors (Schmieden et al., 1993; Shrivastava et al., 2011; Maric et al., 2011), knowledge regarding the nature of such an interaction is limited. The data presented in this study provided several lines of evidence that primary hyperekplexic point mutations in the GlyR α_1 subunit can suppress GABA$_A$R functioning by hijacking GABA$_A$Rs via protein interaction both *in vitro* and *in vivo*. This interaction underlies the pathological mechanism of hyperekplexia (Figure 8). First, hyperekplexic mutations in GlyR α_1 subunits impair the functioning of both GlyRs and GABA$_A$Rs in HEK293 cells and the mouse brainstem hypoglossal nucleus. Second, the mutant GlyRs are highly capable of forming hetero-oligomers with certain types of GABA$_A$Rs. The R271Q point mutation increased the binding free energy, contact surface area, and number of hydrogen bonds between GABA$_A$Rα_1 and GlyRα_1 protein. Third, the signal intensity of such GlyR-GABA$_A$R complexes is highly correlated with the severity of the GABA$_A$R deficiency and exaggerated startle responses in hyperekplexic mice.

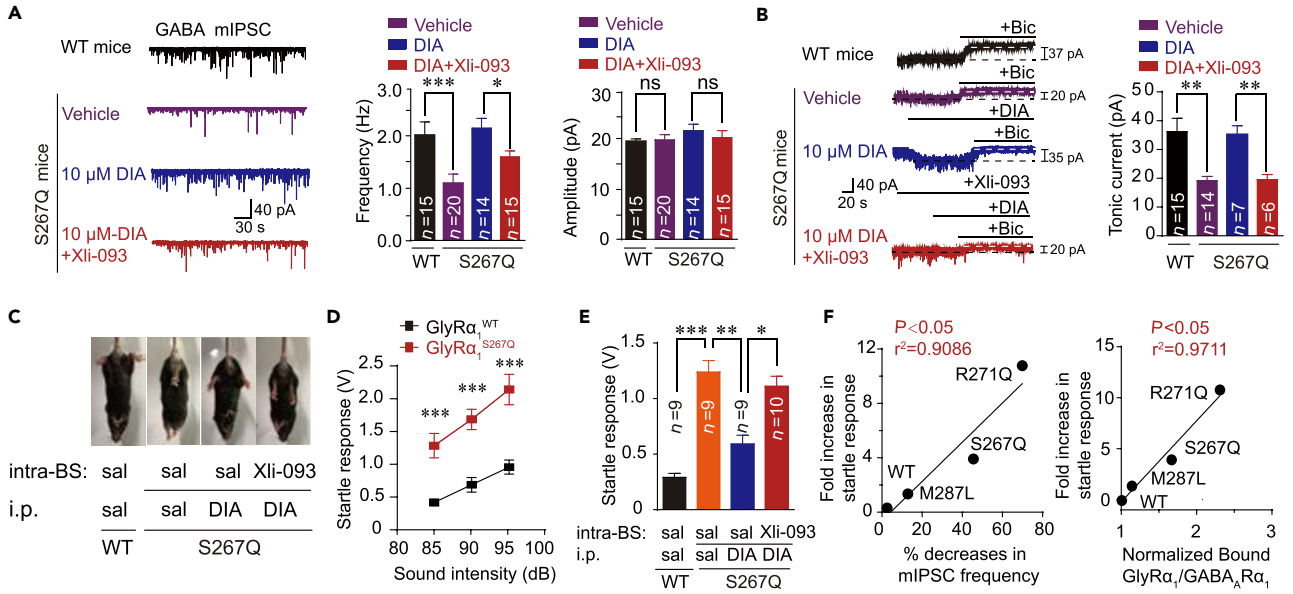

Figure 7. DIA Rescues Dysfunction of Pre- and Extra-synaptic α_5-Containing $GABA_A$Rs and Exaggerated Startle Responses in Hyperekplexic Mutant Mice

(A) Trace records, average frequency, and amplitude of GABAergic mIPSCs in brainstem hypoglossal nucleus slices from WT and GlyR α_1 S267Q mutant mice with or without diazepam (10 μM) and/or Xli-093 (1 μM) pre-incubation.

(B) Trace records and average values of bicuculline-sensitive tonic currents (BSTC) in brainstem hypoglossal nucleus slices from WT and GlyR α_1 S267Q mutant mice with or without diazepam (10 μM) and/or Xli-093 (1 μM) pre-incubation.

(C) Hind feet clenching behavior in GlyRα_1^{S267Q} mutant mice and effect of DIA (i.p. 10 mg/kg) and Xli-093 (intra-brainstem hypoglossal nucleus injection, 5 μg) on this behavior.

(D) Average values of startle responses induced by white noise at 85, 90, and 95 dB in WT (n = 8) and GlyRα_1^{S267Q} (n = 8) mice.

(E) Average values of startle response activated by white noise at 85 dB in WT and GlyRα_1^{S267Q} mutant mice with or without diazepam (i.p. 10 mg/kg) and/or Xli-093 (intra-brainstem hypoglossal nucleus injection, 5 μg) treatments.

(F) Correlation analysis of fold increases in startle response, percentage decreases in mIPSC frequency, and amount of mutant α_1 GlyRs co-immunoprecipitated with $GABA_A$Rs in hyperekplexic mutant mice.

All digits within the columns represent numbers of cells or mice measured. Data are represented as mean ± SEM. *p < 0.05, **p < 0.01, ***p < 0.001 based on unpaired t tests; ns, not significant (p > 0.05).

In this study, weak binding between the WT GlyRs and $GABA_A$Rs was observed in both the HEK-293 cells and brainstem tissues. This weak bonding is unlikely to affect the functioning of both ion channels because the glycine and GABA-activated currents did not show differences when the WT GlyRs and $GABA_A$Rs were either separately expressed or co-expressed in the HEK-293 cells. In contrast, this weak binding may provide a possible explanation for the synergistic effects of glycine and GABA that have been observed in several previous reports (Li and Yang, 1998; Rogers et al., 2016). For instance, a strong synergistic interaction has been observed between GABA and glycine in acutely isolated crucian carp retina neurons. The co-application of both agonists resulted in much larger responses (current >400 pA) than either GABA or glycine alone (current <20 pA) (Li and Yang, 1998). Another report also demonstrated that GABA and glycine can act synergistically at the spinal cord to generate a tonic inhibition of the micturition reflex pathway (Rogers et al., 2016). However, such bonding between GlyR and $GABA_A$R does not appear to always be a good thing. In fact, the hyperekplexic mutations in GlyR caused stronger binding with $GABA_A$R but remarkably impaired the functioning of both channels.

Site mutations generally attenuate the interaction between two associated proteins (Salpietro et al., 2019; Smets et al., 2017; Bizarro and Meier, 2017). However, our findings reveal an entirely opposite pattern in the modulation of protein-protein interactions, particularly under pathological conditions. For instance, several hyperekplexic site mutations in GlyR α_1, such as R271Q and S267Q, enhance its bonding interaction with $GABA_A$R and therefore induce dysfunction in $GABA_A$R. This mechanism may be universal since a similar pattern has been observed in several previous studies investigating the molecular and cellular mechanisms of various diseases. For instance, the R882H mutation in DNA (cytosine-5-)-methyltransferase 3α (DNMT3A) enhances its binding to polycomb repressive complex 1 (PRC1) protein and causes transcriptional silencing,

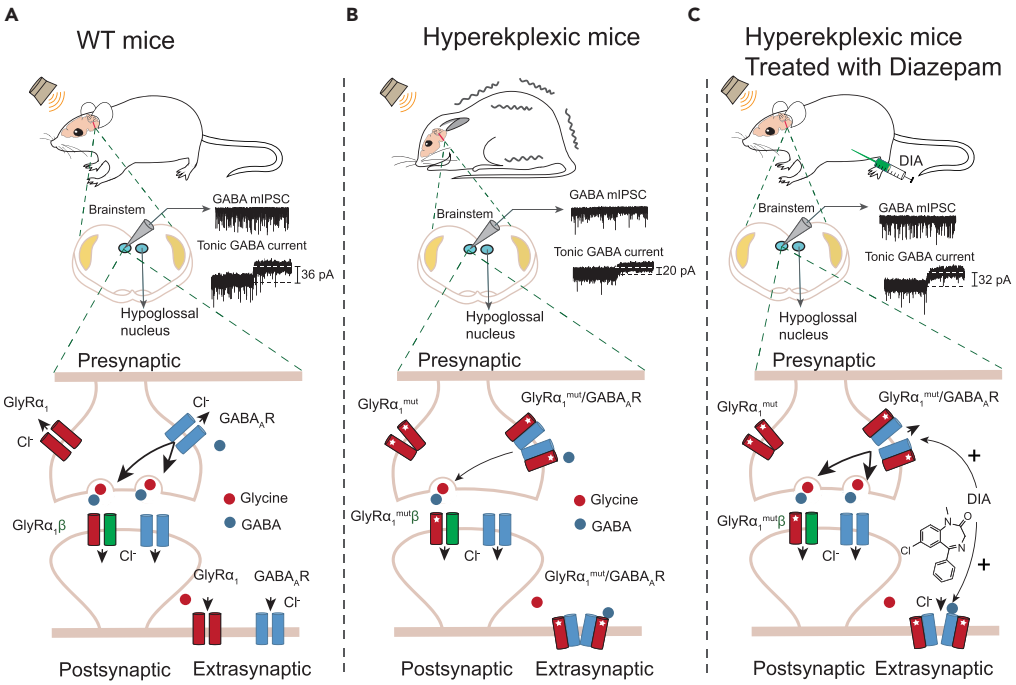

Figure 8. Schematic of Mechanisms in which Hyperekplexic Mutant GlyRs Disrupt Inhibitory Neurotransmission by Interacting with Pre- and Extra-synaptic $GABA_AR$s facilitate

(A) Under normal conditions, presynaptic $GABA_A$Rs facilitate GABA release from GABAergic neuron terminals, activating postsynaptic $GABA_A$Rs to inhibit neurons in the brainstem hypoglossal nucleus. The extra-synaptic $GABA_A$Rs mediate the chronic inhibition of postsynaptic neurons in the brainstem hypoglossal nucleus.

(B) In hyperekplexia disease, the mutant GlyRα_1 binds to pre- and extra-synaptic $GABA_A$Rs and, therefore, reduce GABA release and the chronic inhibition. The postsynaptic GlyRβ subunits prevent the mutant GlyRα_1 from binding to the $GABA_A$Rs.

(C) DIA exerts its therapeutic effect by allosterically potentiating pre- and extra-synaptic α_5-containing $GABA_A$Rs in the brainstem hypoglossal nucleus.

suggesting that PRC1 favors R882 mutants over WT as binding partners in DNMT3A-mutated leukemia disease (Koya et al., 2016). Furthermore, the H443P mutant NOD-like receptor (NLR) protein NLRC4 more strongly interacts with 19S proteasome ATPase Sug1 and ubiquitinated proteins in auto-inflammatory syndrome. This enhanced interaction triggers the constitutive caspase-8-mediated cell death (Raghawan et al., 2017).

The hijacking of $GABA_A$Rs by mutant GlyRs also results in a deficiency in major inhibitory neurotransmission. This finding is consistent with a previous study showing that the R271Q point mutation causes the hyperekplexia phenotype and impairs glycine and GABA transmission in mice (Becker et al., 2002; Von Wegerer et al., 2003). The GlyR β subunit greatly reduces the formation of the GlyR-$GABA_A$R complex, suggesting that the hijacking of the $GABA_A$R by the mutant GlyRα_1 subunits likely occurs in pre- or extra-synaptic sites where the GlyR β subunit is absent. Consistently, the low levels of the GlyR β subunit were associated with the hyperekplexic phenotype in mice (Becker et al., 2000). This hypothesis was tested and supported by the subsequent electrophysiological recordings, which indicated that only pre- and extra-synaptic $GABA_A$Rs were impaired in the brainstem hypoglossal nucleus of hyperekplexic mice. Therefore, this study reveals that the pre- and extra-synaptic $GABA_A$Rs, specifically the α_5 subunit-containing $GABA_A$Rs primarily located in brainstem hypoglossal nucleus, are novel primary targets in hyperekplexia. This hypothesis is supported by our finding that the $GABA_AR\alpha_5$ and GlyRα_1 subunits are colocalized in the brainstem hypoglossal nucleus in GlyRα_1 S267Q and WT mutant mice as revealed by RNAscope technology. DIA, which has been widely used to treat hyperekplexia in the clinic (Garg et al., 2008; Becker et al., 2000; Tijssen et al., 1997), indeed specifically rescued the deficiency of pre- and extra-synaptic α_5-containing $GABA_A$Rs in the HEK-293 cells and mouse brainstem hypoglossal nucleus and restored the exaggerated startle reflex behaviors in the hyperekplexic mutant mice. Thus, developing specific $GABA_AR\alpha_5$ agonists or modulators may be critical for the treatment of hyperekplexia without producing the major psychoactive or sedative side effects that

are associated with benzodiazepines, such as DIA. Such dynamic changes in pre- and extra-synaptic GlyR-$GABA_AR$ complexes may also contribute to various physiological and pathological processes, such as pain, anxiety, and sleep disorders (Botta et al., 2015; Bravo-Hernandez et al., 2016; Crestani et al., 2002; Xiong et al., 2011, 2012). Thus, this GlyR-$GABA_AR$ interaction not only leads to human hyperekplexia but also may contribute to various neurological disorders involving GlyR and $GABA_AR$ deficiency.

Limitations of the Study

Although we identified the interaction between GlyR and $GABA_AR$ in the brain of hyperekplexic transgenic mice, the detailed interaction pattern and interaction sites between both receptors remain unsolved in the present study. Future research should consider utilizing more advanced molecular biology approaches to clarify the detailed mechanisms involved.

METHODS

All methods can be found in the accompanying Transparent Methods supplemental file.

DATA AND CODE AVAILABILITY

The raw data that support the findings of this study are available from the corresponding authors, upon request.

SUPPLEMENTAL INFORMATION

Supplemental Information can be found online at https://doi.org/10.1016/j.isci.2019.08.018.

ACKNOWLEDGMENTS

We thank Yuri Blednov and Adron Harris (University of Texas at Austin, Texas) for providing the α1 S267Q and α1 M287L mutant mice. We thank Hans Weiher (University of Applied Sciences Bonn-Rhein-Sieg, Germany) for providing the α1 R271Q mutant mice. We thank Pearce RA (University of Wisconsin Madison) for providing plasmids of $GABA_ARs$. We thank Dr. David Lovinger (National Institute on Alcohol Abused and Alcoholism, National Institutes of Health, USA) for helpful comments on the manuscript. We acknowledge support from National Key R&D Program of China (2016YFC1300500-2, 2014AA020535), National Natural Science Foundation of China (Grants 91849206, 91649121 & 81901157), the Strategic Priority Research Program of the Chinese Academy of Sciences (Grant XDPB1005), the Fundamental Research Funds for the Central Universities, the Major Program of Development Foundation of Hefei Center for Physical Science and Technology (2017FXZY006), CAS Interdisciplinary Innovation Team (JCTD-2018-20), and Users with Excellence Program/Project of Hefei Science Center CAS.

AUTHOR CONTRIBUTIONS

W.X. initiated, designed, and supervised the project; G.Z., Q.C., and H.P. conducted electrophysiological recordings. G.Z. conducted western blot experiments; K.C., Y.G., and D.L. conducted molecular dynamic simulation; L.Z. conducted *in situ* hybridization using RNAscope; G.Z., X.Z., and Y.H. conducted animal behavioral tests; T.P. synthesized Xli-093; G.Z. and W.X. analyzed data; W.X. and G.Z. wrote the manuscript.

DECLARATION OF INTERESTS

The authors declare no competing interests.

Received: November 20, 2018
Revised: July 16, 2019
Accepted: August 8, 2019
Published: September 27, 2019

REFERENCES

Becker, L., Hartenstein, B., Schenke, J., Kuhse, J., Betz, H., and Weiher, H. (2000). Transient neuromotor phenotype in transgenic spastic mice expressing low levels of glycine receptor β-subunit: an animal model of startle disease. Eur. J. Neurosci. *12*, 27–32.

Becker, L., Von Wegerer, R., Schenkel, J., Zeilhofer, H.U., Swandulla, D., and Weiher, H. (2002). Disease-specific human glycine receptor α1 subunit causes hyperekplexia phenotype and impaired glycine- and $GABA_A$-receptor transmission in transgenic mice. J. Neurosci. *22*, 2505–2512.

Betz, H., Kuhse, J., Schmieden, V., Malosio, M.L., Langosch, D., Prior, P., Schmitt, B., and Kirsch, J. (1991). How to build a glycinergic postsynaptic membrane. J. Cell Sci. Suppl. *15*, 23–25.

Bizarro, J., and Meier, U.T. (2017). Inherited SHQ1 mutations impair interaction with NAP57/dyskerin, a major target in dyskeratosis congenita. Mol. Genet. Genomic Med. *5*, 805–808.

Bode, A., and Lynch, J.W. (2014). The impact of human hyperekplexia mutations on glycine receptor structure and function. Mol. Brain *7*, 2.

Botta, P., Demmou, L., Kasugai, Y., Markovic, M., Xu, C., Fadok, J.P., Lu, T., Poe, M.M., Xu, L., Cook, J.M., et al. (2015). Regulating anxiety with extrasynaptic inhibition. Nat. Neurosci. *18*, 1493.

Bravo-Hernandez, M., Corleto, J.A., Barragan-Iglesias, P., Gonzalez-Ramirez, R., Pineda-Farias, J.B., Felix, R., Calcutt, N.A., Delgado-Lezama, R., Marsala, M., and Granados-Soto, V. (2016). The α5 subunit containing $GABA_A$ receptors contribute to chronic pain. Pain *157*, 613–626.

Brickley, S.G., and Mody, I. (2012). Extrasynaptic $GABA_A$ receptors: their function in the CNS and implications for disease. Neuron *73*, 23–34.

Castro, A., Aguilar, J., Gonzalez-Ramirez, R., Loeza-Alcocer, E., Canto-Bustos, M., Felix, R., and Delgado-Lezama, R. (2011). Tonic inhibition in spinal ventral horn interneurons mediated by α5 subunit-containing $GABA_A$ receptors. Biochem. Biophys. Res. Commun. *412*, 26–31.

Clayton, T., Poe, M.M., Rallapalli, S., Biawat, P., Savic, M.M., Rowlett, J.K., Gallos, G., Emala, C.W., Kaczorowski, C.C., Stafford, D.C., et al. (2015). A review of the updated pharmacophore for the α5 GABAA benzodiazepine receptor model. Int. J. Med. Chem. *2015*, 430248.

Crestani, F., Keist, R., Fritschy, J.M., Benke, D., Vogt, K., Prut, L., Bluthmann, H., Mohler, H., and Rudolph, U. (2002). Trace fear conditioning involves hippocampal α5-$GABA_A$ receptors. Proc. Natl. Acad. Sci. U S A *99*, 8980–8985.

Delgado-Lezama, R., Loeza-Alcocer, E., Andres, C., Aguilar, J., Guertin, P., and Felix, R. (2013). Extrasynaptic $GABA_A$ receptors in the brainstem and spinal cord: structure and function. Curr. Pharm. Des. *19*, 4485–4497.

Dijk, J.M., and Tijssen, M.A. (2010). Management of patients with myoclonus: available therapies and the need for an evidence-based approach. Lancet Neurol. *9*, 1028–1036.

Dray, A., and Straughan, D.W. (1976). Benzodiazepines: GABA and glycine receptors on single neurons in the rat medulla. J. Pharm. Pharmacol. *28*, 314–315.

Essrich, C., Lorez, M., Benson, J.A., Fritschy, J.M., and Luscher, B. (1998). Postsynaptic clustering of major $GABA_A$ receptor subtypes requires the γ 2 subunit and gephyrin. Nat. Neurosci. *1*, 563–571.

Galanopoulou, A.S. (2008). GABA(A) receptors in normal development and seizures: friends or foes? Curr. Neuropharmacol. *6*, 1–20.

Garg, R., Ramachandran, R., and Sharma, P. (2008). Anaesthetic implications of hyperekplexia–'startle disease'. Anaesth. Intensive Care *36*, 254–256.

Hauser, J., Rudolph, U., Keist, R., Mohler, H., Feldon, J., and Yee, B.K. (2005). Hippocampal alpha5 subunit-containing $GABA_A$ receptors modulate the expression of prepulse inhibition. Mol. Psychiatry *10*, 201–207.

Hruskova, B., Trojanova, J., Kulik, A., Kralikova, M., Pysanenko, K., Bures, Z., Syka, J., Trussell, L.O., and Turecek, R. (2012). Differential distribution of glycine receptor subtypes at the rat calyx of Held synapse. J. Neurosci. *32*, 17012–17024.

Huang, X., Chen, H., and Shaffer, P.L. (2017). Crystal structures of human GlyRα3 bound to ivermectin. Structure *25*, 945–950.

Jacob, T.C., Moss, S.J., and Jurd, R. (2008). GABA(A) receptor trafficking and its role in the dynamic modulation of neuronal inhibition. Nat. Rev. Neurosci. *9*, 331–343.

Jia, F., Pignataro, L., Schofield, C.M., Yue, M., Harrison, N.L., and Goldstein, P.A. (2005). An extrasynaptic GABAA receptor mediates tonic inhibition in thalamic VB neurons. J. Neurophysiol. *94*, 4491–4501.

Jonas, P., Bischofberger, J., and Sandkühler, J. (1998). Corelease of two fast neurotransmitters at a central synapse. Science *281*, 419–424.

Koya, J., Kataoka, K., Sato, T., Bando, M., Kato, Y., Tsuruta-Kishino, T., Kobayashi, H., Narukawa, K., Miyoshi, H., Shirahige, K., et al. (2016). DNMT3A R882 mutants interact with polycomb proteins to block haematopoietic stem and leukaemic cell differentiation. Nat. Commun. *7*, 10924.

Langosch, D., Becker, C.M., and Betz, H. (1990). The inhibitory glycine receptor: a ligand-gated chloride channel of the central nervous system. Eur. J. Biochem. *194*, 1–8.

Langosch, D., Thomas, L., and Betz, H. (1988). Conserved quaternary structure of ligand-gated ion channels: the postsynaptic glycine receptor is a pentamer. Proc. Natl. Acad. Sci. U S A *85*, 7394–7398.

Li, P., and Yang, X.L. (1998). Strong synergism between $GABA_A$ and glycine receptors on isolated carp third-order neurons. Neuroreport *9*, 2875–2879.

Lorenzo, L.E., Barbe, A., Portalier, P., Fritschy, J.M., and Bras, H. (2006). Differential expression of GABAA and glycine receptors in ALS-resistant vs. ALS-vulnerable motoneurons: possible implications for selective vulnerability of motoneurons. Eur. J. Neurosci. *24*, 1506.

Lorenzo, L.E., Russier, M., Barbe, A., Fritschy, J.M., and Bras, H. (2007). Differential organization of gamma-aminobutyric acid type A and glycine receptors in the somatic and dendritic compartments of rat abducens motoneurons. J. Comp. Neurol. *504*, 112–126.

Macdonald, R., and Barker, J.L. (1978). Benzodiazepines specifically modulate GABA-mediated postsynaptic inhibition in cultured mammalian neurones. Nature *271*, 563–564.

Maric, H.M., Mukherjee, J., Tretter, V., Moss, S.J., and Schindelin, H. (2011). Gephyrin-mediated gamma-aminobutyric acid type A and glycine receptor clustering relies on a common binding site. J. Biol. Chem. *286*, 42105–42114.

McCracken, L.M., Lowes, D.C., Salling, M.C., Carreau-Vollmer, C., Odean, N.N., Blednov, Y.A., Betz, H., Harris, R.A., and Harrison, N.L. (2017). Glycine receptor α 3 and α2 subunits mediate tonic and exogenous agonist-induced currents in forebrain. Proc. Natl. Acad. Sci. U S A *114*, E7179–E7186.

Miller, P.S., and Aricescu, A.R. (2014). Crystal structure of a human $GABA_A$ receptor. Nature *512*, 270–275.

Muller, E., Triller, A., and Legendre, P. (2004). Glycine receptors and GABA receptor alpha 1 and gamma 2 subunits during the development of mouse hypoglossal nucleus. Eur. J. Neurosci. *20*, 3286–3300.

Muller, E., Corronc, L., Triller, A., and Legendre, P. (2006). Developmental dissociation of presynaptic inhibitory neurotransmitter and postsynaptic receptor clustering in the hypoglossal nucleus. Mol. Cell. Neurosci. *32*, 254–273.

Nemecz, A., Prevost, M.S., Menny, A., and Corringer, P.J. (2016). Emerging molecular mechanisms of signal transduction in pentameric ligand-gated ion channels. Neuron *90*, 452–470.

Pribilla, I., Takagi, T., Langosch, D., Bormann, J., and Betz, H. (1992). The atypical M2 segment of the beta subunit confers picrotoxinin resistance to inhibitory glycine receptor channels. EMBO J. *11*, 4305–4311.

Raghawan, A.K., Sripada, A., Gopinath, G., Pushpanjali, P., Kumar, Y., Radha, V., and Swarup, G. (2017). A disease-associated mutant of NLRC4 shows enhanced interaction with SUG1 leading to constitutive FADD-dependent caspase-8 activation and cell death. J. Biol. Chem. *292*, 1218–1230.

Rogers, M.J., Shen, B., Reese, J.N., Xiao, Z.Y., Wang, J.C., Lee, A., Roppolo, J.R., Groat, W.C., and Tai, C.F. (2016). Role of glycine in nociceptive and non-nociceptive bladder reflexes and pudendal afferent inhibition of these reflexes in cats. Neurourol. Urodyn. *35*, 798–804.

Salpietro, V., Malintan, N.T., Llano-Rivas, I., Spaeth, C.G., Efthymiou, S., Striano, P., Vandrovcova, J., Cutrupi, M.C., Chimenz, R., David, E., et al. (2019). Mutations in the neuronal vesicular SNARE VAMP2 affect synaptic membrane fusion and impair human neurodevelopment. Am. J. Hum. Genet. *104*, 721–730.

Schmieden, V., Kuhse, J., and Betz, H. (1993). Mutation of glycine receptor subunit creates beta-alanine receptor responsive to GABA. Science *262*, 256–258.

Shiang, R., Ryan, S.G., Zhu, Y.Z., Hahn, A.F., O'Connell, P., and Wasmuth, J.J. (1993). Mutations in the α1 subunit of the inhibitory glycine receptor cause the dominant neurologic disorder, hyperekplexia. Nat. Genet. *5*, 351–358.

Shrivastava, A.N., Triller, A., and Sieghart, W. (2011). GABAA receptors: post-synaptic co-localization and cross-talk with other receptors. Front. Cell. Neurosci. *5*, 7.

Singer, J.H. (2008). GABA is an endogenous ligand for synaptic glycine receptors. Neuron *57*, 475–477.

Smets, M., Link, S., Wolf, P., Schneider, K., Solis, V., Ryan, J., Meilinger, D., Qin, W., and Leonhardt, H. (2017). DNMT1 mutations found in HSANIE patients affect interaction with UHRF1 and neuronal differentiation. Hum. Mol. Genet. *26*, 1522–1534.

Snodgrass, S.R. (1978). Use of 3H-muscimol for GABA receptor studies. Nature *273*, 392–394.

Thomas, R.H., Chung, S.K., Wood, S.E., Cushion, T.D., Drew, C.J., Hammond, C.L., Vanbellinghen, J.F., Mullins, J.G., and Rees, M.I. (2013). Genotype-phenotype correlations in hyperekplexia: apnoeas, learning difficulties and speech delay. Brain *136*, 3085–3095.

Tijssen, M.A., Schoemaker, H.C., Edelbroek, P.J., Roos, R.A., Cohen, A.F., and vanDijk, J.G. (1997). The effects of clonazepam and vigabatrin in hyperekplexia. J. Neurol. Sci. *149*, 63–67.

Turecek, R., and Trussell, L.O. (2001). Presynaptic glycine receptors enhance transmitter release at a mammalian central synapse. Nature *411*, 587–590.

Von Wegerer, J., Becker, K., Glockenhammer, D., Becker, C.M., Zeilhofer, H.U., and Swandulla, D. (2003). Spinal inhibitory synaptic transmission in the glycine receptor mouse mutant spastic. Neurosci. Lett. *345*, 45–48.

Waldvogel, H.J., Biggins, F.M., Singh, A., Arasaratnam, C.J., and Faull, R.L.M. (2019). Variable colocalisation of GABAA receptor subunits and glycine receptors on neurons in the human hypoglossal nucleus. J. Chem. Neuroanat. *97*, 99–111.

Wojcik, S.M., Katsurabayashi, S., Guillemin, I., Friauf, E., Rosenmund, C., Brose, N., and Rhee, J.S. (2006). A shared vesicular carrier allows synaptic corelease of GABA and glycine. Neuron *50*, 575–587.

Xiong, W., Cheng, K.J., Cui, T.X., Godlewski, G., Rice, K.C., Xu, Y., and Zhang, L. (2011). Cannabinoid potentiation of glycine receptors contributes to cannabis-induced analgesia. Nat. Chem. Biol. *7*, 296–303.

Xiong, W., Cui, T.X., Cheng, K.J., Yang, F., Chen, S.R., Willenbring, D., Guan, Y., Pan, H.L., Ren, K., Xu, Y., et al. (2012). Cannabinoids suppress inflammatory and neuropathic pain by targeting alpha 3 glycine receptors. J. Exp. Med. *209*, 1121–1134.

Xiong, W., Chen, S.R., He, L.M., Cheng, K.J., Zhao, Y.L., Chen, H., Li, D.P., Homanics, G.E., Peever, J., Rice, K.C., et al. (2014). Presynaptic glycine receptors as a potential therapeutic target for hyperekplexia disease. Nat. Neurosci. *17*, 232–239.

ISCI, Volume *19*

Supplemental Information

Human Hyperekplexic Mutations in Glycine Receptors Disinhibit the Brainstem by Hijacking $GABA_A$ Receptors

Guichang Zou, Qi Chen, Kai Chen, Xin Zuo, Yushu Ge, Yiwen Hou, Tao Pan, Huilin Pan, Dan Liu, Li Zhang, and Wei Xiong

Supplemental Figures

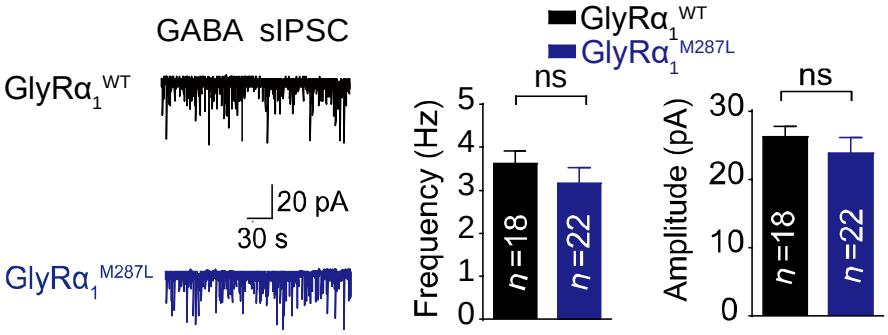

Figure S1. Trace records, average frequency and amplitude of GABAergic sIPSCs in brain-stem hypoglossal nucleus slices from WT and GlyRα$_1^{M287L}$ mutant mice (related to Figure 1). All digits within the columns represent numbers of cells measured. Data are represented as mean ± SEM. ns, not significant ($P > 0.05$) based on unpaired t-tests.

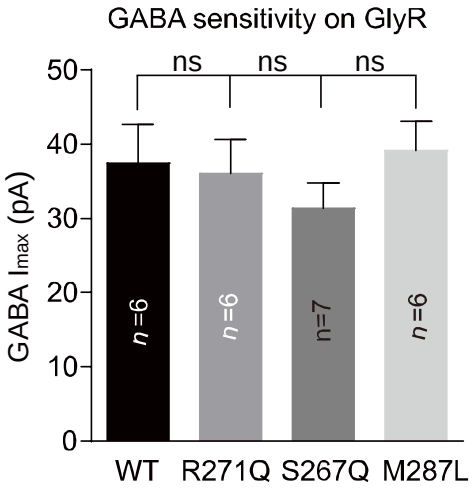

Figure S2. GABA-activated currents on GlyRs (related to Figure 2). Average values of currents activated by 1 mM GABA in HEK-293 cells expressing WT and mutant α_1 GlyRs. All digits within the columns represent numbers of cells measured. Data are represented as mean ± SEM. ns, not significant ($P > 0.05$) based on unpaired t tests.

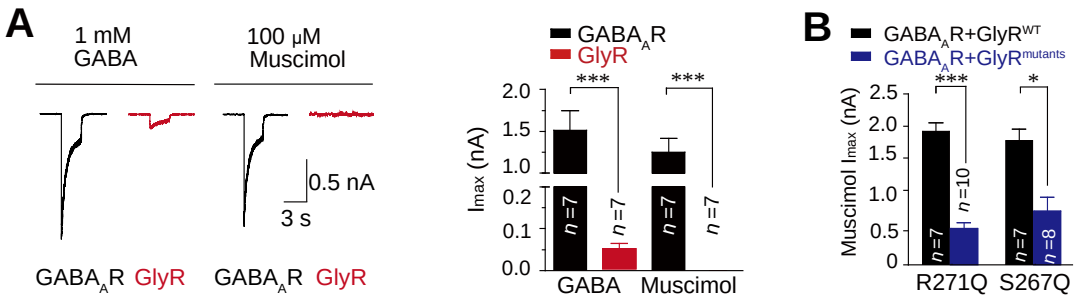

Figure S3. Effects of hyperekplexic mutations of GlyRα$_1$ on the currents activated by muscimol (related to Figure 2). (A) Trace records and average values of GABA and muscimol I_{max} in HEK-293 cells expressing GABA$_A$Rs ($\alpha_1\beta_2\gamma_2$) and GlyRs separately. **(B)** Average values of muscimol I_{max} activated by 100 μM muscimol in HEK-293 cells co-expressing GABA$_A$Rs ($\alpha_1\beta_2\gamma_2$) and mutant α_1 GlyRs. All digits within the columns represent numbers of cells measured. Data are represented as mean ± SEM. * $P < 0.05$, *** $P < 0.001$ based on unpaired t tests.

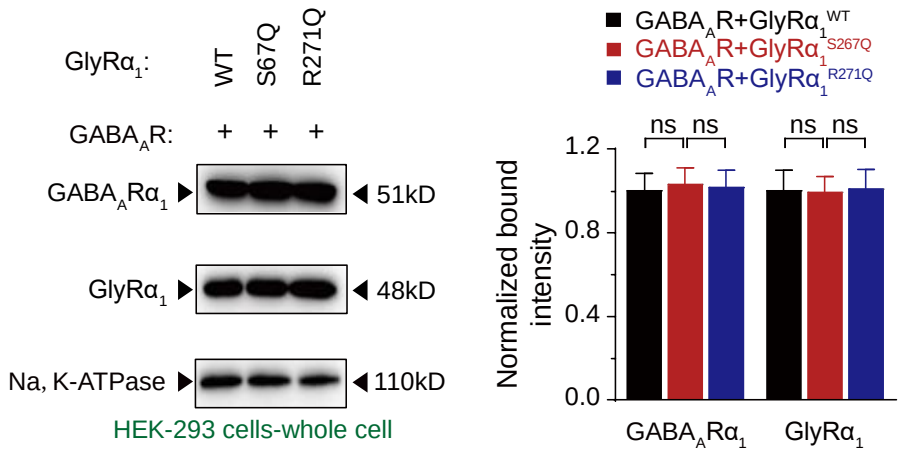

Figure S4. (related to Figure 3). Western blotting results showing protein expression levels of GlyR and $GABA_AR$ in plasma membranes extracted from HEK-293 cells co-transfected with the cDNA of $GlyR\alpha_1^{WT}$, $GlyR\alpha_1^{R271Q}$ and $GlyR\alpha_1^{S267Q}$ with $GABA_ARs$ ($\alpha_1\beta_2\gamma_2$). ns, not significant ($P > 0.05$) based on unpaired t tests.

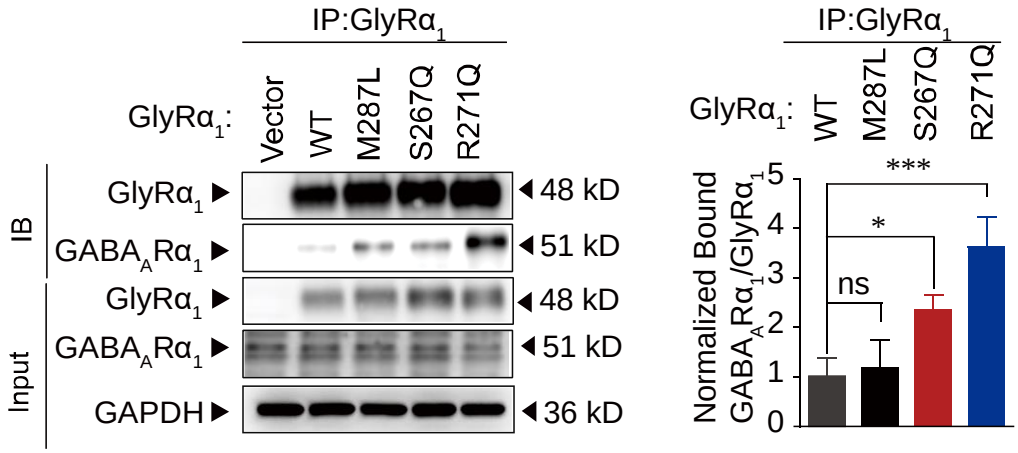

Figure S5. (related to Figure 3). The $GABA_AR\alpha_1$ was purified using $GlyR\alpha_1$ antibodies in HEK-293 cells co-expressing $GABA_ARs$ ($\alpha_1\beta_2\gamma_2$) and WT/mutant $GlyR\alpha_1$, and co-precipitating proteins were detected by immunoblotting. Inputs are immunoblots of the same protein in cell lysates prior to co-IP. Quantification of WT and mutant $GlyR\alpha_1$ binding to $GABA_AR\alpha_1$. All digits within the columns represent numbers of cells measured. Data are represented as mean ± SEM. * $P < 0.05$, *** $P < 0.001$; ns, not significant ($P > 0.05$) based on unpaired t tests.

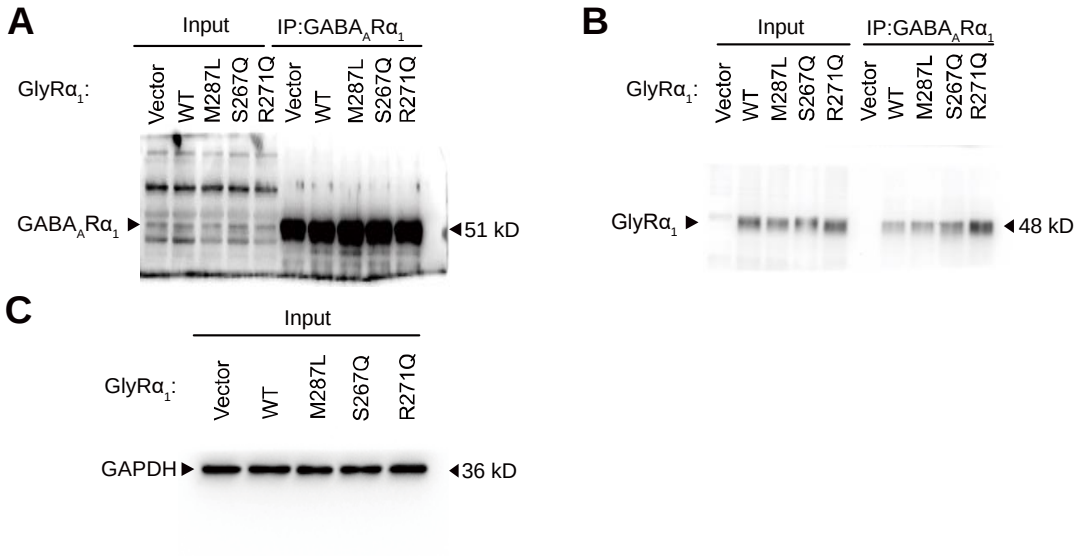

Figure S6. Whole gel images for Figure 3A (A-C) (related to Figure 3).

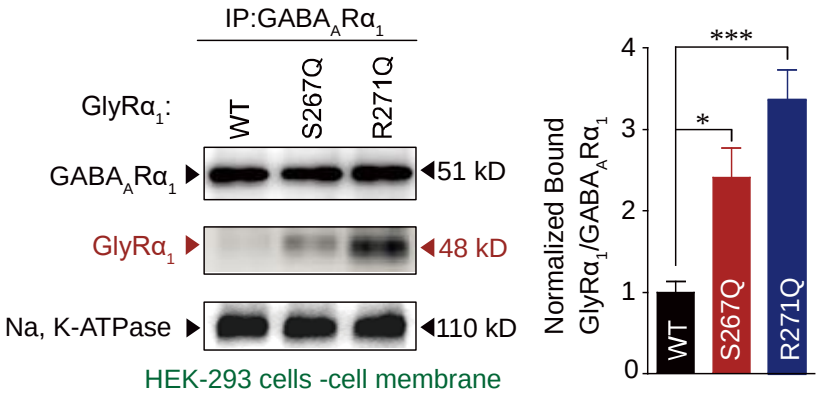

Figure S7. Identification of association between mutant GlyRα$_1$ and GABA$_A$Rα$_1$ in the plasma membrane (related to Figure 3). Plasma membrane GlyR α$_1$ was purified using GABA$_A$R α$_1$ antibodies in HEK-293 cells co-expressing GABA$_A$Rs ($\alpha_1\beta_2\gamma_2$) and WT/mutant α$_1$ GlyRs, and the co-precipitating proteins were detected by immunoblotting. Quantification of WT and mutant GlyR α$_1$ binding to GABA$_A$R α$_1$ (n = 3). The data were normalized to the WT group. Data are represented as mean ± SEM. * $P < 0.05$, *** $P < 0.001$ based on unpaired t tests.

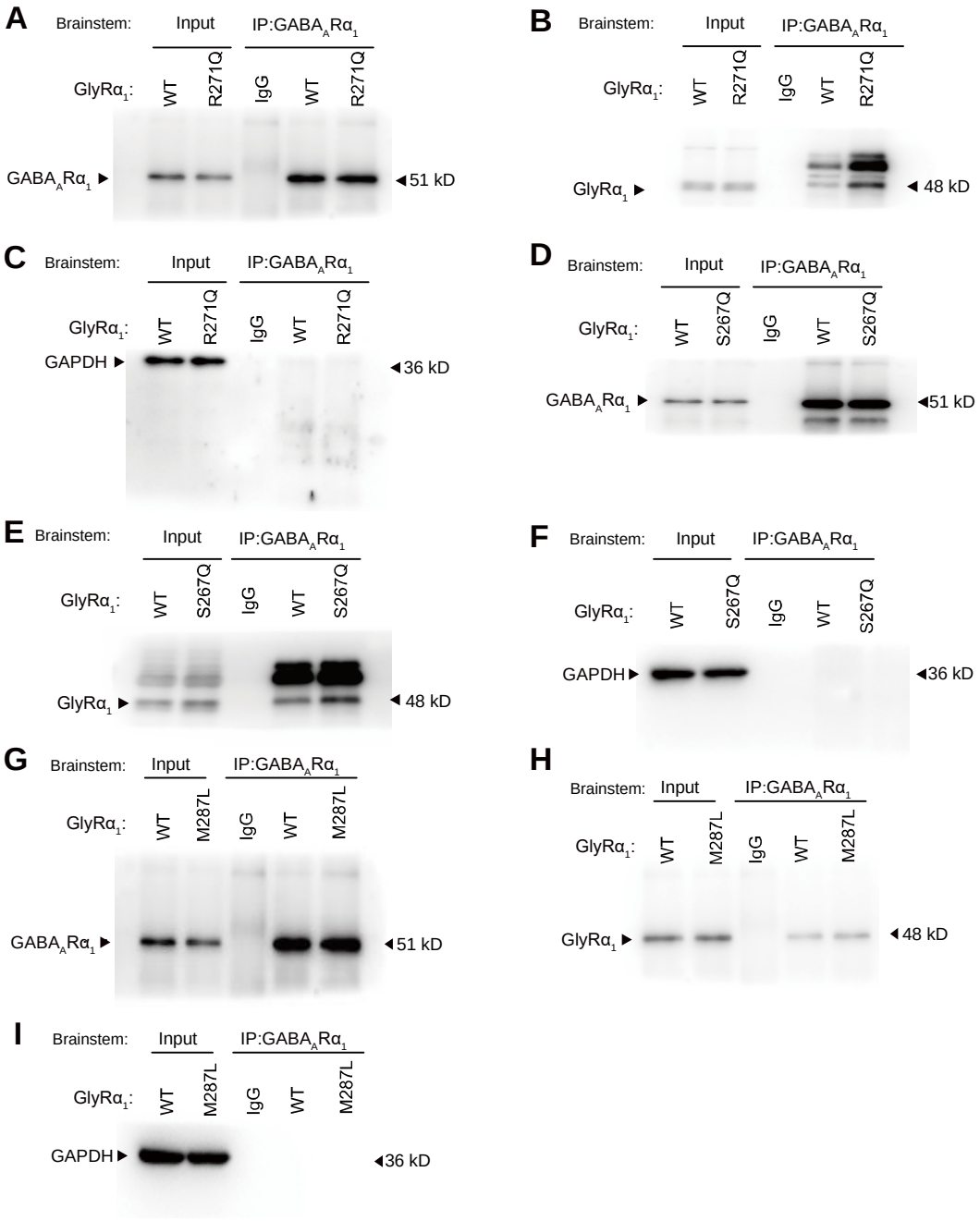

Figure S8. Whole gel images for Figure 3B (A-C); whole gel images for Figure 3C (D-F) and whole gel images for Figure 3D (G-I) (related to Figure 3).

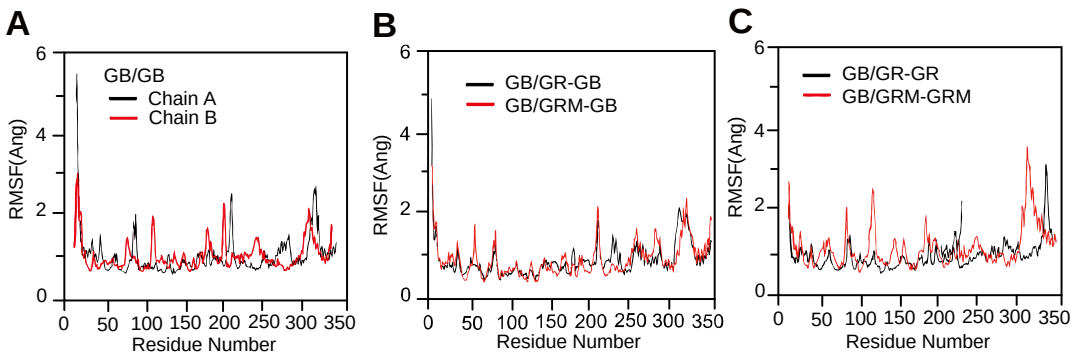

Figure S9. Root mean square fluctuation (RMSF) of three protein systems with respect to the starting structure (related to Figure 4). (A-C) Preparation and Molecular dynamic simulation of three protein bound systems. Protonation status of residues in three systems: Four histidine residues (His107, His 119, His 191 and His267 in chain A) and four histidine residues (His107, His 119, His 191 and His267 in chain B) were protonated at Nε in GB/GB system. Four histidine residues (His107, His 119, His 191 and His267 in chain A) and three histidine residues (His109 , His 201 and His215 in chain B) were protonated at Nε in GB/GR system. Four histidine residues (His107, His 119, His 191 and His267 in chain A) and three histidine residues (His109 , His 201 and His215 in chain B) were protonated at Nε in GB/GRM system. All other residues were configured under the standard protonation states at pH 7.

The optimization of the solvent, equilibration of the whole systems and the molecular dynamic simulation of the equilibrated systems were conducted following the steps listed below: After applying a position restraint of 100 mol−1 Å−2 on all solute atoms, solvent and ions were optimized by three steps: a. energy minimization for 1000 cycles; b. dynamic simulation of 10ps with the temperature increased from 10K to 298K; c. dynamic simulation of 10ps under pressure of 1 bar to equilibrate the density. After applying a restraint weight of 2.0 mol−1 Å−2 on proteins, the whole systems were equilibrated. First, 1000 cycles of energy minimization were applied. Second, the temperature was increased from 10K to 298 K over a period of 5ps dynamic simulation. Third, a dynamic simulation of 200ps under the constant pressure of 1 bar was applied. Finally, the whole system was equilibrated by 100ps dynamic simulation under constant temperature of 298 K and pressure of 1 bar. 1 ns MD production simulations were carried out under the constant temperature and pressure of 298K and 1 bar. Periodic boundary conditions were applied in the NPT ensemble using langevin dynamics. The SHAKE algorithm was applied to fix all bond lengths involving hydrogen atoms. A time step of 2 fs and a direct non-bond interaction cut off radius of 8.0 Å were used with particle-mesh Ewald for long-range electrostatic interactions. Three parallel runs were carried out for each system.

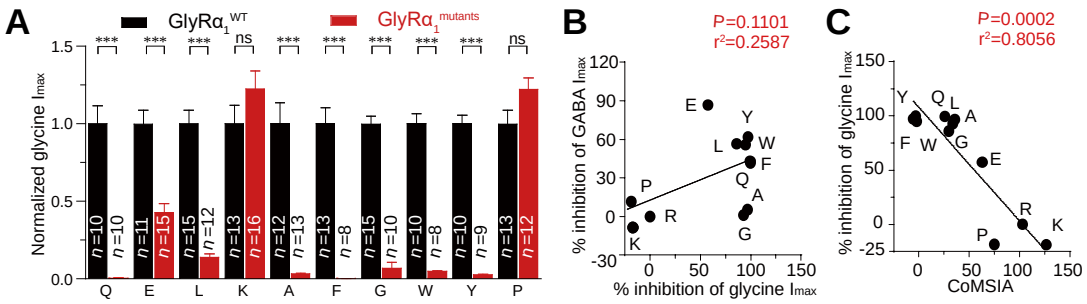

Figure S10. Mutagenesis and correlation analysis of GlyRα$_1^{R271}$ site (related to Figure 4).

(A) The average values of glycine I_{max} activated by 1 mM glycine in HEK-293 cells expressing various R271 site mutant GlyRα$_1$ subunits. All data were normalized to their respective controls (WT group). All digits within the columns represent numbers of cells measured. Data are represented as mean ± SEM. *** $P < 0.001$; ns, not significant ($P > 0.05$) based on unpaired t tests.

(B) Correlation analysis of R271 mutations-induced percentage inhibition of glycine and GABA I_{max} (linear regression).

(C) Correlation analysis of CoMSIA values of various amino acids at 271 and percentage inhibition of glycine I_{max} (linear regression).

Residues used for 3D-QSAR analysis were generated in SYBYL8.1 software. The structures were minimized and charged with MMFF94 force field. Comparative molecular similarity index analysis (CoMSIA) was conducted to model the correlation between residues structures and inhibition activity. Both electrostatic field and steric field were generated. Final computed CoMSIA value of residues were plotted with inhibition activity.

Figure S11. Whole gel images for Figure 4G (related to Figure 4).

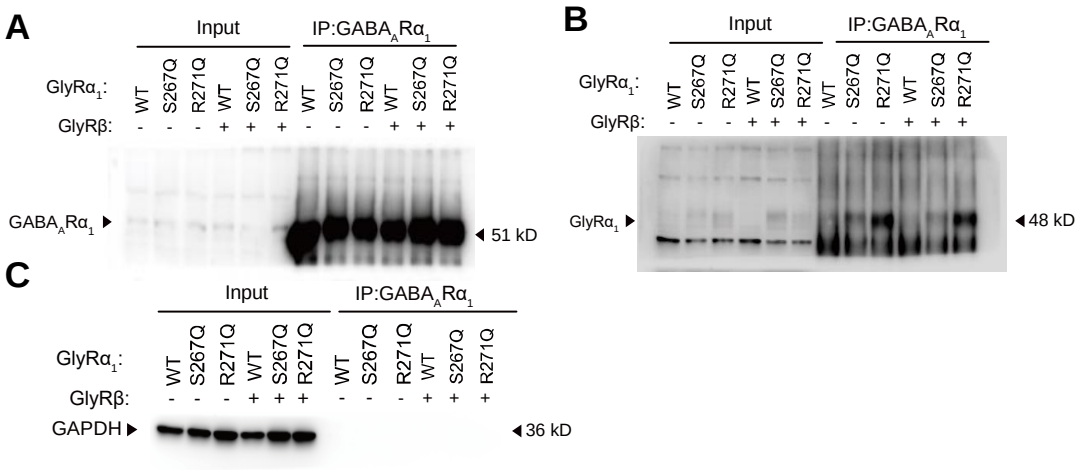

Figure S12. Whole gel images for Figure 5C (related to Figure 5).

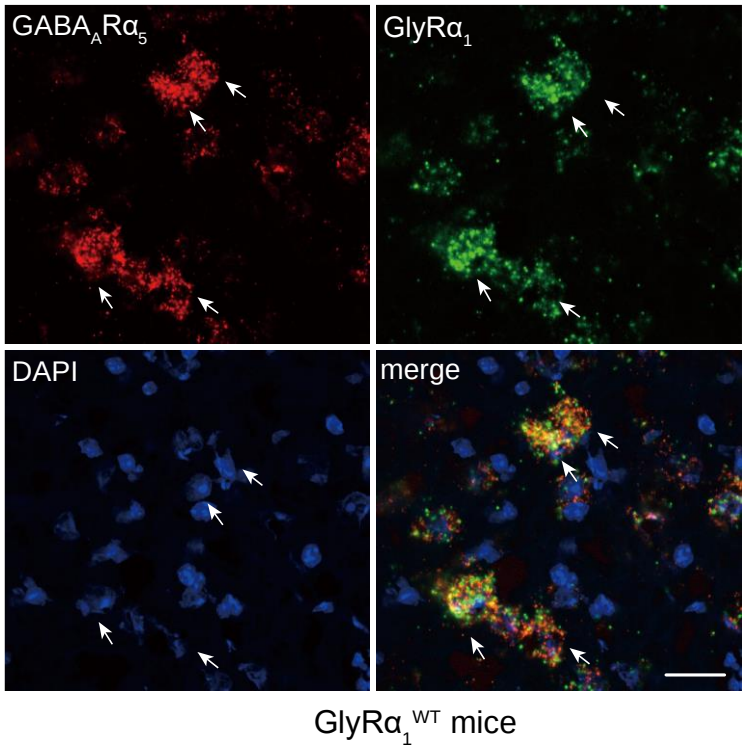

Figure S13. (related to Figure 6). Representative confocal imaging showing colocalization of $GABA_ARα_5$ and $GlyRα_1$ subunits mRNAs in the $GlyRα_1^{WT}$ mouse brainstem hypoglossal nucleus using RNAscope technology. Scale bar, 25µm.

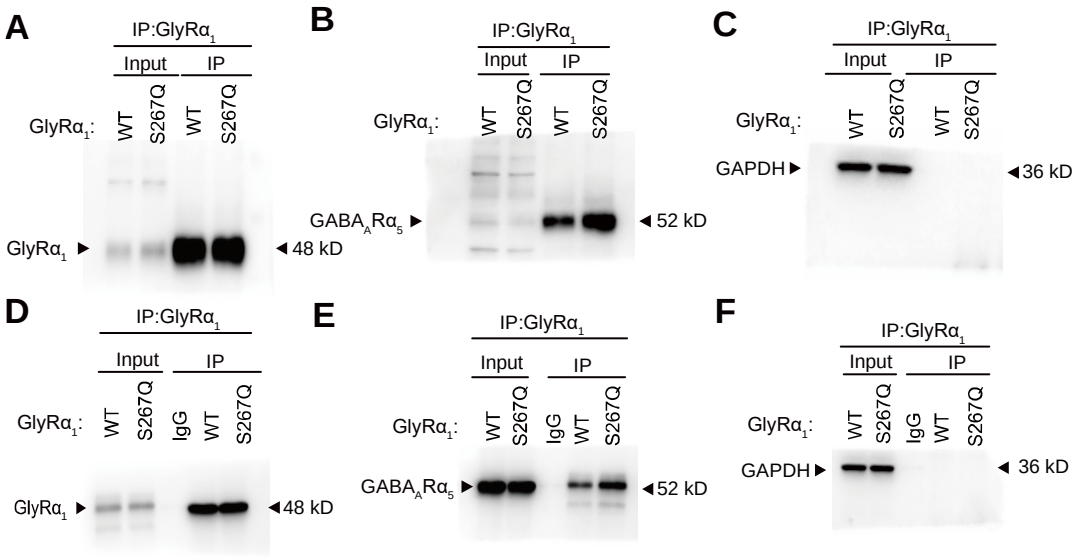

Figure S14. Whole gel images for Figure 6D (A-C) and whole gel images for Figure 6E (D-F) (related to Figure 6).

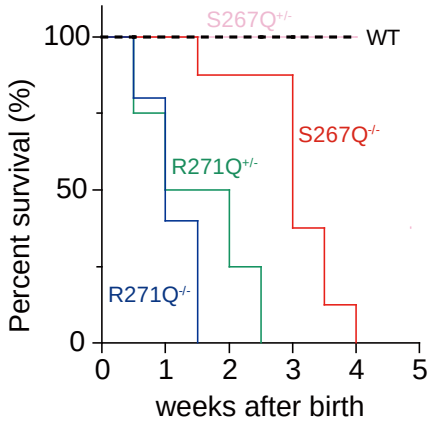

Figure S15. Survival curves of WT, S267Q and R271Q GlyRα$_1$ mutant transgenic mice (related to Figure 7) (WT, n= 6; R271Q$^{+/-}$, n=4; R271Q$^{-/-}$, n=6; S267Q$^{-/-}$, n=8; S267Q$^{+/-}$, n=6). All R271Q$^{+/-}$, R271Q$^{-/-}$ and S267Q$^{-/-}$ mice died within 4 weeks of life.

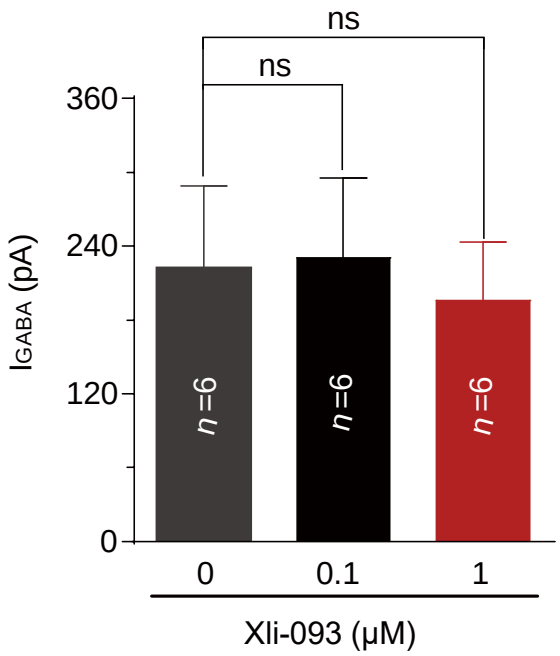

Figure S16. Average values of currents activated by 1 μM GABA in HEK-293 cells with or without pre-incubation of 0.1 or 1 μM Xli-093 in HEK-293 cells expressing $GABA_ARs$ ($\alpha_5\beta_2\gamma_2$) (related to Figure 7). All digits within the columns represent numbers of cells measured. Data are represented as mean ± SEM. ns, not significant ($P > 0.05$) based on unpaired t tests.

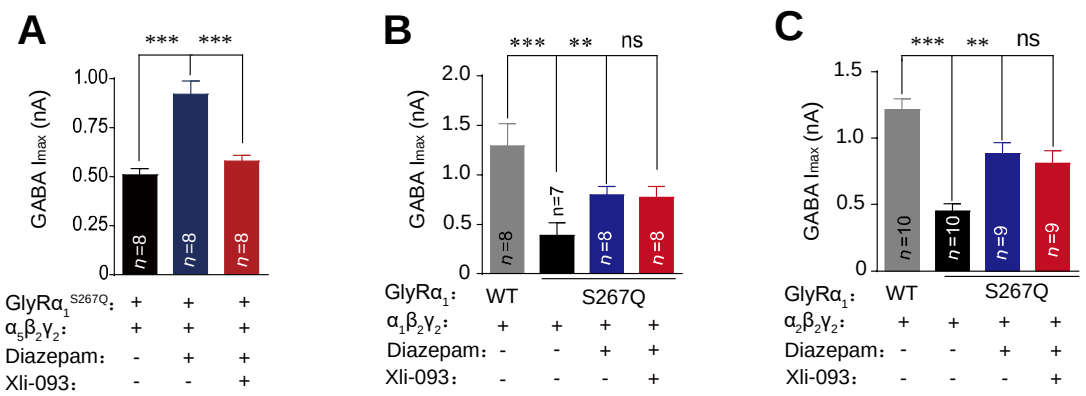

Figure S17. Effects of Xli-093 on diazepam-induced potentiation of $GABA_A$Rs (related to Figure 7). (A-C) Average values of currents activated by 1 mM GABA in HEK-293 cells co-expressing $GlyR\alpha_1^{S267Q}$ and α_5- **(A)**, α_1- **(B)** or α_2- **(C)** containing $GABA_A$Rs with or without pre-incubation of 10 μM diazepam and 1 μM Xli-093. All digits within the columns represent numbers of cells measured. Data are represented as mean ± SEM. $^{**}P < 0.01$, $^{***}P < 0.001$; ns, not significant ($P > 0.05$) based on unpaired t tests.

Transparent Methods

Animals.

GlyRα_1^{S267Q} and GlyRα_1^{M287L} transgenic mice were from Yuri Blednov and Adron Harris (University of Texas at Austin, Texas) (Findlay et al., 2003; Borghese et al., 2012). GlyRα_1^{R271Q} transgenic mice were from Hans Weiher (University of Applied Sciences Bonn-Rhein-Sieg, Germany) (O'Shea et al., 2004). Hyperekplexic GlyR mutant mice and their wild-type littermates (P12-P21) were used in all recording, western blot and co-immunoprecipitation experiments. Hyperekplexic GlyR mutant mice and their wild-type littermates (7-8 weeks old) were used in startle reflex and RNAscope tests. All mice were housed under a semi-natural dark/light cycle of 12:12 h. All genetically engineered mice studied were homozygous and heterozygous for the mutant α_1 subunit. Genotyping of the α_1 M287L mutant mice was done using the following primers: forward: 5′-GAATCTTCCAGGCAACATTTCAG-3′; reverse: 5′-AGTATCCCACCAAGCC AGTCTTT-3′. Genotyping of the α_1 S267Q mutant mice were done using the following primers: forward: 5′-GCTTTAACTTCTGCCCTATGG-3′; reverse: 5′-GTTGTTGTTAACTTGTTTATTG-3′. Genotyping of the α_1 R271Q mutant mice was done using the following primers: forward: 5′-CTCATCTTTGAGTGGCAGG A-3′; reverse: 5′-GCATCCATGTTGAT CCAGAA-3′. Wild-type littermates and mutant (α_1 M287L, α_1 S267Q and α_1 R271Q) homozygous mice used for the electrophysiological recording were produced from heterozygous breeding pairs. Mice used in this study are all male unless otherwise indicated. All procedures were approved by the Institutional Animal Use and Care Committee of School of Life Sciences, University of Science & Technology of China.

Site-directed mutagenesis.

All point mutations for $\alpha_{1\text{-}3}$ GlyR were introduced using a QuikChange Site-Directed Mutagenesis kit (Takara, Inc.). Sequence of DNA mutants were confirmed through double-stranded DNA sequencing with Genetic Analysis System (Sangon, Inc.).

Electrophysiological recording.

HEK-293 cells (ATCC) were cultured using Dulbecco`s Modified Eagle Media with 10 % fetal bovine serum in 37°C and 5 % CO2. Cells were plated at a density of 10^6 cells/ml in 35-mm dishes and allowed to grow to 70 % confluence before transfection (Hu et al., 2006). Plasmids coding $GABA_A$ R and GlyR were co-transfected into HEK-293 cells using Lipofectamine 2000 (Invitrogen) reagents. 2 days after transfection, electrophysiological recordings were carried out. HEK-293 cells were treated with 0.25 % (w/v) Trypsin 2 hours before recording. HEK-293 cells were then lifted and recorded with external solution containing 140 mM NaCl, 5 mM KCl, 2.0 mM $CaCl_2$, 1.0 mM $MgCl_2$, 10 mM glucose and 10 mM HEPES (pH 7.4 with NaOH, ~320 mOsm with sucrose). Patch pipettes (3–5 MΩ) were filled with intracellular solution contained 140 mM CsCl, 4 mM $MgCl_2$, 10 mM EGTA, 10 mM HEPES, 0.5 mM Na-GTP and 2 mM Mg-ATP (pH 7.2 with CsOH, ~280 mOsm). Membrane currents were recorded in the whole-cell configuration using an Axopatch 200B amplifier (Axon) at 20–25 °C. Cells were held at –60 mV unless otherwise indicated. Data were acquired using pClamp 10.4 software (Molecular Devices, Sunnyvale, CA). Drugs were applied using a Warner fast-step stepper motor–driven system.

Brainstem hypoglossal nucleus slice preparation and recording.

For brainstem slice neuron recording, hyperekplexic GlyR mutant mice and their wild-type littermates (P12-P21) were used. Brainstem slices were prepared as followings: parasagittal brainstem slices (260-µm thick) were prepared from P_{12} to P_{21} mice with Leica Vibratome in ice-cold cutting solution containing (in mM) 30 NaCl, 26 $NaHCO_3$, 10 glucose, 194 sucrose, 4.5 KCl, 1.2 NaH_2PO_4, 1 $MgCl_2$ and continuously bubbled with carbogen (95 % O_2-5 % CO_2). Slices were transferred to a perfusion chamber containing artificial cerebrospinal fluid (ACSF) (in mM): 124 NaCl, 4.5 KCl, 1 $MgCl_2$, 2 $CaCl_2$, 1.2 NaH_2PO_4, and 26 $NaHCO_3$, continuously bubbled in carbogen. After 60 min recovery at room temperature, slices were transferred to a recording chamber continuously perfused with ACSF (2-3ml/min). All recordings were performed at 34 °C using glass pipettes filled with internal solution containing 120 mM CsCl, 4 mM $MgCl_2$, 10 mM EGTA, 10 mM HEPES, 0.5 mM Na-GTP and 2 mM Mg-ATP (pH 7.2 with CsOH,

~280 mOsm). For sIPSCs recording, 4 mM kynurenic acid and 1 μM strychnine were added in continuously perfused ACSF solution. For mIPSCs recording, 10 μM TTX was additionally added in continuously perfused ACSF. Maximum current of $GABA_ARs$ induced by 1mM GABA was recorded in brainstem slices of $GlyR\alpha_1$ mutant mice and littermate wild type mice. Extra-synaptic current of $GABA_ARs$ was recorded with bicuculline. 80 μM bicuculline,10 μM Diazepam and 1 μM Xli-093 was applied by puff application directly to the recorded neuron using a positive pressure system (4 PSI, 15 ms; Toohey Company, Fairfield, NJ). The input resistance was monitored continuously, and the recording was abandoned if the resistance changed more than 15 %. All brainstem slice recordings were performed under a double-blind condition.

Computational investigation of three protein bound systems.

Three protein bound systems were prepared to investigate the binding affinity between $GABA_AR$ and GlyR. Crystal structures of protein $GABA_AR\ \beta_3$ obtained at a 2.7 Å resolution (Miller et al., 2014) (PDB ID: 4COF) and protein GlyR α_3 obtained at a 2.5 Å resolution (Huang et al., 2017) (PDB ID: 5VDH) were obtained from the RCSB Protein Data Bank (RCSB PDB: www.rcsb.org). Each system contains the following two chains: GB/GB - two chains (A; B) extracted from the crystal structure of $GABA_AR\ \beta_3$ (PDB ID: 4COF); GB/GR - one chain (A) extracted from the $GABA_AR$ and one chain extracted (A) from the GlyR; GB/GRM – same complex as GB/GR, except for Arg271 of GlyR is mutated to Glutamine. The initial binding conformation of the GB/GR complex was obtained using Z-dock software (Pierce et al., 2014).

All crystallographic water molecules and ligands were removed. The protonation states were investigated using the H++ Server (Anandakrishnan et al., 2012) (protonation status is listed in Supporting Information). The protein was charged using an AMBER ff12SB force field. The proteins were solvated in a rectangular box of TIP3P water with a minimum distance between the protein and the box edge of 11 Å. The initial density of the systems was set as 0.9 $g \cdot mL^{-1}$.

The optimization of the solvent, equilibration of the whole systems and the molecular dynamic simulation of the equilibrated systems were conducted in all three systems.

The trajectory was sampled every 1 ps for the analysis using the ptraj and cpptraj programs. The protein structures and snapshots were visualized using VMD (Humphrey et al., 1996). The RMSF values of the protein systems were calculated after aligning to the first structure during the entire 1 ns. Using the MM/GBSA (Molecular Mechanics/Generalized Born Surface Area) method, the binding free energy of two chains was calculated during the entire simulation time. The distances between the residue and atom pairs were obtained using the WORDOM program (Seeber et al., 2007) and mapped using the Gnuplot program (http://www.gnuplot.info/).

Western blotting.

The GlyR and $GABA_AR$ plasmids were transfected into HEK-293 cells using lipo2000 (Invitrogen) reagents. After 48–72 h, whole cell proteins were prepared using buffer containing 1 M Tris-HCL (pH 7.5), 1 % protease inhibitor cocktail (Roche), 1 M NaCl and 5 % sodium deoxycholate. The membrane protein was collected using a Membrane Protein Extraction Kit (89842, Thermo Fisher) according to the manufacturer's instructions. Equal amounts of protein were loaded on 12 % SDS-PAGE gels and transferred to PVDF membranes (NEN, Boston, MA, USA) for 90 min. After the transfer, the membranes were blocked by incubation with TBS containing 0.1 % Tween-20 and 5 % (wt/vol) nonfat milk for 1 h and with primary antibodies against $GABA_AR$ α_1 (1:100, 06-868, Merck), $GABA_AR$ α_5 (1:500, ab10098, Abcam), GlyR α_1 (1:500, NB300-113, Novus), GAPDH (1:5000, 60004-1-AP, Proteintech), and Na, K-ATPase (1:1000, #3010, CST) overnight. After three 5-min washes with TBS plus Tween-20, the membranes were incubated with secondary antibodies against rabbit (1:5000, ab6721, Abcam) or mouse (1:5000, ab6789, Abcam) for 1 h at room temperature. The membranes were washed three times with TBS plus Tween-20 for 5 min, and the protein bands were imaged using ECL reagent (Thermo Fisher Scientific). For western blot analysis of tissue samples, hyperekplexic GlyR mutant mice and their wild-type littermates (P12-P21) were used. The other procedures were consistent with those used for the HEK-293 cells.

Co-Immunoprecipitation.

The cell lysates were collected using methods similar to those used for the Western blotting. To show whether there is any change in protein expression level, 60 μL cell or tissue lysates was extracted and mixed with same volume loading buffer as input before immunoprecipitation. The "input" always performed as a necessary control in all co-immunoprecipitation experiments. IgG-agarose beads were incubated with primary antibodies against $GABA_AR$ α_1 or GlyR α_1 protein overnight at 4°C. The mixture was washed and centrifuged 5 times for 1 min at 12,000 rpm with PBS. The samples were collected, and the centrifugal mixture with the cell lysates was blended and then incubated overnight. After washing and centrifuging the mixtures 5 times for 1 min with cell lysis buffer, 100 μL loading buffer were added, and then the mixture was boiled for 5 min. The samples and inputs were then used for the SDS-PAGE and Western blotting analysis. The primary antibodies were the same as those used in the Western blotting analysis. A mouse anti-rabbit IgG (light-chain specific) (L57A3) mAb reacting with the light chain of rabbit IgG was used to confirm the specific protein band. Normal rabbit IgG (sc-2027, Santa Cruz) was used as a negative control in the immunoprecipitation experiments. For co-immunoprecipitation of tissue samples, hyperekplexic GlyR mutant mice and their wild-type littermates (P12-P21) were used. To completely grind the tissue samples, an automatic lapping machine and ultrasonic homogenizers were used. The other procedures were consistent with those used for the HEK-293 cells.

RNAscope method.

For RNAscope tests, hyperekplexic GlyR mutant mice and their wild-type littermates (7-8 weeks old) were used. Whole brain tissues were removed and frozen on dry ice. The fresh frozen tissue sections (12 μm thick) were mounted on positively charged microscopic glass slides (Thermo Fisher Scientific, Waltham, MA). Both the GlyRα_1 (Glra1) RNA probe (NM_001290821) and $GABA_AR\alpha_5$ subunit (GABra5) probe (NM_176942) were designed and provided by Advanced Cell Diagnostics, Inc. (Hayward, CA). The experimental procedures followed the manufacturer's instructions of RNAscope Fluorescent Multiplex V2 Assay. Stained slides were cover-slipped with fluorescent mounting medium (ProLong Gold Antifade Reagent, P36930, Thermo Fisher

Scientific, Waltham, MA) and scanned using Zeiss LSM880 confocal microscope (Zeiss, USA, San Diego, CA). For each sample, three adjacent sections were stained using the Glra1 and GABra5 RNAscope probes. "GlyRα_1 mRNA–positive neurons and $GABA_AR\alpha_5$ mRNA–positive neurons were counted using ImageJ software (National Institutes of Health, NIH. https://imagej.nih.gov/ij/). The percentage of GlyRα_1 mRNA–positive neurons that co-expressing $GABA_AR\alpha_5$ mRNA were calculated using the following formula: Proportion of $GABA_AR\alpha_5^+$ neurons among GlyRα_1^+ neurons (%) = amount of neurons expressing both $GABA_AR\alpha_5$ and GlyRα_1 / amount of neurons expressing GlyRα_1 alone. The percentage of $GABA_AR\alpha_5$ mRNA–positive neurons that co-expressing GlyRα_1 mRNA were calculated using the following formula: Proportion of GlyRα_1^+ neurons among $GABA_AR\alpha_5^+$ neurons (%) = amount of neurons expressing both $GABA_AR\alpha_5$ and GlyRα_1 / amount of neurons expressing $GABA_AR\alpha_5$ alone."

The synthesis of Xli-093.

Xli-093 were synthesized according to a previous study (Li et al., 2003) as shown in the following steps. A solution of carbonyldiimidazole (90.7 mg, 0.56 mmol) and 8-ethynyl-5,6-dihydro-5-methyl-6-oxo-4H-imidazo[l,5-a][l,4]-benzod iazepi-ne-3-car-boxylic acid (148.9 mg, 0.53 mmol) in anhydrous DMF (10 mL) was stirred for 3 h at room temperature. After the starting material was converted by TLC (silica gel), to the solution was then added 1,3-propanediol (21.3 mg, 0.28 mmol) and DBU (102.1 mg, 0.67 mmol) in dry DMF (1 mL). The mixture was stirred at room temperature over night until the reaction was complete by TLC (silica gel). The reaction mixture was then poured into water (60 mL) and extracted with DCM (3 × 50 mL). The combined organic layer was washed with water (50 mL), brine and dried with Na_2SO_4. The solu-tion was filtered and the filtrate was condensed. The residue was purified by flash chro-matography (silica gel, EtOAc/ petroleum ether (60-90°C), 1:2) to provide Xli-093 (81.3 mg) as a white solid in 51 % yield. 1H NMR (400 MHz, CDCl3): δ 8.19 (2H, d), 7.90 (2H, s), 7.73 (2H, dd), 7.41 (2H, d), 5.29-5.15 (2H, br), 4.56 (4H, t), 4.37 (2H, br), 3.26 (6H, s), 3.24 (2H, s), 2.42-2.27 (2H, m).

Drugs.

Most chemicals including GABA and glycine were achieved from Sigma-Aldrich. All solutions were prepared the day before experiment with ultrapure water. Agonist, modulator and antagonist were diluted before experiment with external solution or ACSF. Diazepam and Xli-093 was dissolved in ethanol before further dilution by external solution. Diazepam was sourced from Sigma-Aldrich. All the final concentration of ethanol in working solution was less than 8 mM, which had no potential effect on I_{Gly} and I_{GABA}. All the vehicles used in experiments had no latency responses when used alone.

Startle reflex test.

The mice were placed in Med Associates Startle Reflex System (Med Associates Inc.) chambers and allowed to habituate for 5 min. Then, the mice were tested to measure their level of startle using a series of pseudorandom white noise startle stimuli (10 presentations of each sound intensity, 85 dB, 90 dB, and 95 dB) with a 58-63 s inter-trial interval (ITI). Male heterozygous S267Q transgenic mice and their wild-type littermates (7–8 weeks old) were used in the startle test. The mice were injected with diazepam (10 mg/kg, i.p.) and Xli-093 (5 μg/2 μL, intra-brainstem hypoglossal nucleus.) before being placed in the startle device.

Statistical analysis.

In our study, no statistical methods were used to predetermine sample sizes, all experiments and data analysis were conducted in a blinded way. For behavioral experiments, animals from different genotypes were picked randomly for testing. For electrophysiological experiments, brainstem hypoglossal neurons or transfected HEK-293 cells were randomly picked for patch-clamp recordings. Statistical analysis of the concentration-response data is performed with the use of a nonlinear curve-fitting program. Data were fit using the Hill equation, I/I_{max} = bottom + (top − bottom)/(1 + 10^(logEC_{50} − log[agonist]) × Hill slope), where I is the current amplitude activated by a given concentration of agonist ([agonist]), *Imax* is the maximum response of the cell, and EC_{50} is the concentration eliciting a half-maximal response. Correlation analysis were performed with linear regression. Data were statistically compared by unpaired t test using GraphPad Prism 6.0 (GraphPad Software), as indicated in the specific figure legends. Average

values are expressed as the mean ± SEM and mean ± SD. $P < 0.05$ was considered significant. The data distribution was assumed to be normal, but this was not formally tested.

Supplemental References

Anandakrishnan, R., Aguilar, B., and Onufriev, A.V. (2012). H++ 3.0: automating pK prediction and the preparation of biomolecular structures for atomistic molecular modeling and simulations. Nucleic Acids Res. *40*, W537-W541.

Borghese, C.M., Blednov, Y.A., Quan, Y., Iyer, S.V., Xiong, W., Mihic, S.J., Zhang, L., Lovinger, D.M., Trudell, J.R., Homanics, G.E., and Harris, R.A. (2012). Characterization of two mutations, M287L and Q266I, in the α1 glycine receptor subunit that modify sensitivity to alcohols. J. Pharmacol. Exp. Ther. *340*, 304–316.

Findlay, G.S., Phelan, R., Roberts, M.T., Homanics, G.E., Bergeson, S.E., Lopreato, G.F., Mihic, S.J., Blednov, Y.A., and Harris, R.A. (2003). Glycine receptor knock-in mice and hyperekplexia-like phenotypes: comparisons with the null mutant. J. Neurosci. *23*, 8051-8059.

Huang, X., Chen, H., and Shaffer, P.L. (2017). Crystal Structures of Human GlyRα3 Bound to Ivermectin. Structur*e 25*, 945-950.

Humphrey, W., Dalke, A., and Schulten, K. (1996). VMD: visual molecular dynamics. J. Mol. Graph. *14*, 33-38.

Hu, X.Q., Sun, H., Peoples, R.W., Hong, R., and Zhang, L. (2006). An interaction involving an arginine residue in the cytoplasmic domain of the 5-HT3A receptor contributes to receptor desensitization mechanism. J. Biol. Chem. *28*, 21781-21788.

Li, X.Y., Cao, H., Zhang, C.C., Furtmueller, R., Fuchs, K., Huck, S., Sieghart, W., Deschamps, J., and Cook, J.M. (2003). Synthesis, in vitro affinity, and efficacy of a bis 8-ethynyl-4H-imidazo[1,5a]-[1,4]benzodiazepine analogue, the first bivalent alpha 5 subtype selective BzR/$GABA_A$ antagonist. J. Med. Chem. *46*, 5567-5570.

Miller, P.S., and Aricescu, A.R. (2014). Crystal structure of a human $GABA_A$ receptor. Nature *512*, 270-275.

O'Shea, S.M., Becker, L., Weiher, H., Betz, H., and Laube, B. (2004). Propofol restores the function of "hyperekplexic" mutant glycine receptors in Xenopus oocytes and mice. J. Neurosci. *24*, 2322-2327.

Pierce, B.G., Hellman, L.M., Hossain, M., Singh, N.K., Vander-Kooi, C.W., Weng, Z.,

and Baker, B.M. (2014). Computational design of the affinity and specificity of a therapeutic T cell receptor. Plos. Comput. Biol. *10*, e1003478.

Seeber, M., Cecchini, M., Rao, F., Settanni, G., and Caflisch, A. (2007). Wordom: a program for efficient analysis of molecular dynamics simulations. Bioinformatics *23*, 2625-2627.